國立臺灣大學生物資源暨農學院生物科技研究所

碩士論文

Institute of Biotechnology
College of Bioresource and Agriculture
National Taiwan University
Master Thesis

利用基因編輯與體外RISC分析研究蘚苔植物與被子植物微型核酸調控機制

The investigation for miRNA machinery in bryophyte and angiosperm through CRISPR gene editing and *in vitro* RISC assay

楊芊燕

Qian Yuan Yong

指導教授：林詩舜 博士

Advisor: Shih-Shun Lin, Ph.D.

中華民國 112 年 8 月

August, 2023

doi:10.6342/NTU202303945

Acknowledgement

First of all, tons of thanks to my advisor, Prof. Shih-Shun Lin who is being very patience and gave me a lot of encouragements throughout this one and half years, especially these few months when I am writing this thesis. It is an impossible process for me if without encouragement from Prof. Lin. Nonetheless, thanks to all of the committee members, Dr. Tzyy-Jen Chiou, Dr. Ho-Ming Chen, and Dr. Jun-Yi Yang for their time and willingness to come through typhoon and join my oral defence as committee. At the same time, gratitude to my head of department, Prof. Shau-Pin Lin for being very kind and supportive when I was facing my nationality problems. Also to member of NTU OIA members, and Legislator Mei-Ling Luo and her office members who helped me a lot when I was facing problem that could have withdrawn my study in NTU.

Special thanks to be given to my friends and seniors for being very kind and helpful throughout my one and half year; Syuan-Fei for her to guide me with her expertise in all experiment, Yu-Ling, listen to my problems when I was being stressful, Wei-Lun, who guide my western blot even after I have been here for one year, and Pookie, who give me a lot of helps and her guidance on my RISC assay, also my juniors, Shiuan-Cheng, who always willing to help me on doing any experiment and help me feeding rabbit when I have no free time, Yu-Ju, always helps me sub-culture my mutants and preparing my medium plate, Liang-He, who take over material ordering for lab daily usage, and Chao-Tzu who always so cheerful and working so hard in lab.

doi:10.6342/NTU202303945

中文摘要

基因沉默是個植物中為抵禦微生物或面對環境改變時常見的處變機制。Dicer-like 4 (DCL4) 是植物體中負責切割核糖核酸並產生可與 Argonaute 1 蛋白(AGO1)結合之短干擾核糖核酸 (short interfering RNA, siRNA)，反式作用干擾小核糖核酸 (trans-acting siRNA)，或病毒小核糖核酸(viral small RNA)。Hyponastic Leaves 1 (HYL1) 蛋白是個雙股核糖核酸連接蛋白，是小分子核糖核酸(microRNA, miRNA)生產路徑中一個重要的調節蛋白。AGO1 為核糖核酸誘導沉默複合物(RNA-induced silencing complex, RISC)的重要組合物之一，已被證明在地錢中會被 MIR11707 所調控。常間回文重複序列叢集關聯蛋白(Clustered Regularly Interspaced Short Palindromic Repeat/ CRISPR associated protein 9, CRISPR-Cas9）基因編輯技術在此研究中被應用於變異地錢及阿拉伯介中相關的調節者。另外，葡萄球菌核酸酶样 tudor 结构域蛋白 1 (Tudor-SN, TSN)，捲曲葉蛋白(Curly leaf, CLF)，和類異染色質蛋白 1 (Like Heterochromatin Protein 1, LHP1)皆為植物調節機制中的重要調節者，TSN 與信使核糖核酸(messenger RNA, mRNA)的去帽路徑相關，CLF 和 LHP1 則與阿拉伯介的開花相關。因此，我們假設這些蛋白質可以它們的專有方式影響 AGO1 的功能。協同性蛋白水解酶 (helper-component proteinase; HC-Pro) 是個來自馬鈴薯 Y 病毒屬的 RNA 沉默抑制蛋白，它可以影響被感染的植物體內核糖核酸誘導沉默複合物的活動。爲了瞭解 HC-Pro 和 AGO1 之間的聯係，我們的前輩把 *P1/HC-Pro*^{Tu} 轉植株中的自噬蛋白 ATG8a 去除。在研究的下一步，我們把這個轉植株進行了與 Col-0 的雜交，由此間接把 ATG8a 恢復。此轉植株預計可以恢復 ATG8a 的 AGO1 降解的功能。除此之外，我們也成功製造出 TSN，CLF 和 LHP1 基因的變異植株。在此論文中，我們利用體外核糖核酸誘導沉默複合物活

doi:10.6342/NTU202303945

動測定(in vitro RISC activity assay)研究了 AGO1 蛋白質在各個轉植株及變異植株中的活動。作爲地錢中的模範植物，*Marchantia polymorpha* 在近期植物學研究一直是非常重要的研究模本。利用 CRISPR-Cas9 的技術，通過把向導 RNA (guide RNA, gRNA)片段插入載體並轉入地錢中，我們將 *DCL4, HYL1* 和 *MIR11707* 由 Tak-1 中變異去除。我們將會觀察各變異植株的表性特徵。

關鍵字：小分子核糖核酸，地錢，HYL1，DCL4，AGO1，協同性蛋白水解酶，HC-Pro, *miR11707*, CRISPR/Cas9, TSN, CLF, LHP1, RISC, 基因沉默機制，阿拉伯介

doi:10.6342/NTU202303945

Abstract

Gene silencing is a typical pathway in plants for defending from viruses and environmental changes. Dicer-like 4 (DCL4) is a dicer protein in plant responses to produce short-interfering RNA (siRNA) for trans-acting siRNA (tasiRNA) and viral small RNA that could be loaded into Argonaute 1 (AGO1) for gene silencing, whereas Hyponastic Leaves 1 (HYL1) is a double strand RNA binding protein that is one of the regulators in the microRNA (miRNA) biogenesis pathway. As an essential component in the RNA-induced silencing complex (RISC), AGO1 is also known to be regulated by *miR11707* in *Marchantia polymorpha*. To further investigate the roles of these regulators, CRISPR-Cas9 gene editing has been used to generate knocked-out mutant in Arabidopsis and *M. polymorpha* plants in this study. Moreover, Tudor-SN (TSN), Curly Leaf (CLF), and Like Heterochromatin Protein1 (LHP1) proteins were shown to be important in plant regulatory pathways, whereas TSN related to uncapping of mRNA, CLF, and LHP1 are both related to the flowering of *Arabidopsis thali*ana. So, we hypothesized that they affect AGO1 function in their specific ways. Helper component-proteinase (HC-Pro) is a viral RNA silencing suppressor from potyvirus that will disrupt the RISC activity in the virus-infected plant. To study the relation between HC-Pro and AGO1, our senior produced a *P1/HC-Pro* transgenic line that *ATG8a* is being knocked out simultaneously. As the study's next step, they cross this transgenic line with Columbia (Col-0) to recover the *atg8a* mutant activity. It is expected that, in this transgenic line, the degradation of AGO1 shall be recovered compared to the *atg8a* knocked-out line. We had also successfully mutated *TSN*, *CLF,* and *LHP1* genes in *A. thaliana* Col-0 ecotype. In this thesis, we studied AGO1 protein levels and *in vivo* RISC activity assay in all transgenic lines to confirm the AGO1 activity in those lines. As a model plant in liverwort, *M. polymorpha* has been a critical study model in the plant-related study. With CRISPR-Cas-9, we have

doi:10.6342/NTU202303945

knocked out *DCL4*, *HYL1*, and *MIR11707* genes by inserting a guide RNA (gRNA) fragment in a vector and transferring the vectors into *M. polymorpha* plants. We will be studying their phenotypic symptoms when these regulators are knocked-out successfully.

Keywords: miRNA, *Marchantia polymorpha*, HYL1, DCL4, AGO1, HC-Pro, *miR11707*, CRISPR/Cas9, TSN, CLF, LHP1, RISC, gene silencing, *Arabidopsis thaliana*

doi:10.6342/NTU202303945

Table of Contents

doi:10.6342/NTU202303945

doi:10.6342/NTU202303945

doi:10.6342/NTU202303945

Introduction

The Clustered Regularly Interspaced Short Palindromic Repeats (CRISPR)/ CRISPR-associated endonuclease 9 (Cas9) genome editing system is a highly effective technology, enabling alterations of specific sequences in the genome (Sugano et al., 2018). In consists of two primary components: the Cas9 protein, acting as an RNA-guided endonuclease, and a single guide RNA (gRNA), spanning 18-24 nucleotide (nt) in length, which specifies a target sequence within the genome (Sugano et al., 2018; Tjita, 2021). The Cas9 protein, derived from *Streptococcus pyogenes*, attaches to the protospacer adjacent motif (PAM) sequence, represented by the DNA sequence "NGG". The binding activity triggers an interaction between a gRNA and its target DNA sequence(Sugano et al., 2018; Barman et al., 2020). If the gRNA aligns with the target sequence, the nuclease domains of Cas9 become capable of cleaving the phosphodiester bonds on both sides of the strands, situated 3 bp upstream of the PAM sequence. This can result in the disruption of target locus (Sugano et al., 2018). The CRISPR-Cas9 system has become an extraordinarily powerful technique for gene editing in numerous biochemistry studies (Tjita, 2021).

Gene silencing is a critical pathway that regulates normal growth, development, and defences against viral and bacterial infection (Anandalakshmi et al., 1998; Anders Hafrén, 2018). In response, viruses have evolved a protein known as helper component-Proteinase (HC-Pro) to function as a silencing suppressor (Anandalakshmi et al., 1998; Kasschau et al., 2003; Anders Hafrén, 2018). Our previous study established a transgenic line of *P1/HC-Pro*^{Tu} plant to study the viral supressing pathway, revealing that P1 is a critical component enhancing the phenotype observed in transgenic plant (Lin et al., 2016). The study also found that the level of ARGONAUTE 1 (AGO1) was reduced in *P1/HC-Pro*^{Tu} plants, suggesting abnormal AGO1 degradation might occur during turnip mosaic virus

doi:10.6342/NTU202303945

(TuMV) infection in Arabidopsis. Known for its role in the degradation of long-lived cytosolic proteins and organelles in plant, autophagy may be implicated (Bu et al., 2020; Ying, 2022). The Autophagy-related (ATG) protein 8 (ATG8) is a ubiquitin-like protein central to autophagy (Bu et al., 2020). As demonstrated by Wei et al. (2022), *HC-Pro*^{Tu} directly interacts with ATG8a, but not AGO1, suggesting no direct regulation between *HC-Pro*^{Tu} and AGO1. Instead, ATG8a may be responsible for AGO1 degradation in relation to *P1/HC-Pro*^{Tu} infection. Using the CRISPR-Cas9 technique, we knocked-out ATG8a from *P1/HC-Pro*^{Tu} plant, leading to the recovered of AGO1 levels in the *P1/HC-Pro*^{Tu}*/atg8a*^{ge} plants (Wei et al., 2022). In the current study, to further investigate the relationship between *P1/HC-Pro*^{Tu}, AGO1, and ATG8a, we recovered ATG8a by crossing *P1/HC-Pro*^{Tu}*/atg8a*^{ge} plant with Col-0 plant, generating the *P1/HC-Pro*^{Tu}*/ATG8a* +/+ plant, and evaluating these plants in this study.

Marchantia polymorpha, also known as liverwort, serves as a model species for the study of plant evolution and gene function among basal land plants (Lin et al., 2016; Bowman et al., 2017; Tjita, 2021). Thanks to its short life cycle, ease of propagation and crossing, small genome size, among other advantage, *M. polymorpha* has become one of the most extensively studied species of liverworts (Tjita, 2021). Leveraging the advanced technique reported by Nishihama et al. (2018), we have successfully mutated proteins of interest in *M. polymorpha*. This development opens the door for more in-depth studies involving these mutants.

MicroRNA (miRNA) is a 20-24 nt non-coding RNA that serves as a regulator of post-transcriptional gene silencing (PTGS) (Lin et al., 2016; Tjita, 2021; Wei et al., 2022). It plays a crucial role in regulating stages of plant growth and aid in defense mechanism against viral or bacterial infection (Tjita, 2021). In plants, miRNAs are incorporated into

doi:10.6342/NTU202303945

the AGO1. Along with other components, they form an RNA-induced silencing complex (RISC), possessing the ability to cleave mRNA or inhibit its translation (Re et al., 2020).

Hyponastic leaves 1 (HYL1) is a double stranded RNA (dsRNA)-binding protein (Lu and Fedoroff, 2000; Han et al., 2004; Tjita, 2021). It plays a pivotal role in miRNA biogenesis, contributing to the processing of pri-miRNA into pre-miRNA, and ultimately, to the miRNA/miRNA* duplex (Dong et al., 2008; Tjita, 2021). As such, mutations in HYL1 affect the formation of mature miRNA (Vazquez et al., 2004; Dong et al., 2008), leading to developmental deficiencies in plant (Vazquez et al., 2004). Dicer-like 4 (DCL4) is one of the dicer proteins present in plant that can cleave long dsRNA, typically originating from viral infection (Fukudome and Fukuhara, 2017). It produces short-interfering RNA (siRNA), such as trans-acting siRNA (tasiRNA) and viral small RNA, and loaded into AGO1 for gene silencing (Fukudome and Fukuhara, 2017). In *M. polymorpha*, the role of MpDCL4 has been suggested in siRNA biogenesis; however, there remains a gap in our understanding, particular in relation to genetic or biochemical studies in the Mp*DCL4* gene (Lin and Bowman, 2018).

MIR11707 is a known miRNA in *M. polymorpha* that targeting Mp*AGO1* and regulates Mp*AGO1* expression (Berruezo et al., 2016; Lin et al., 2016; Hong, 2023). Uniquely, it consists of 2 different miRNAs, *MIR11707.1* and *MIR11707.2*, both of which targeting MpAGO1, and originate from the same precursor (Lin et al., 2016; Hong, 2023). A previous study from Hong (2023) showing that the *mir11707*^{ge} mutant exhibits a temperature-dependence phenotype, which becomes apparent under growth conditions of 28°C.

In our previous studies, we produced mutants for Mp*DCL4*, Mp*HYL1*, and Mp*MIR11707* using the spooring method with CRISPR-Cas9 technique (Tjita, 2021;

doi:10.6342/NTU202303945

Hong, 2023). However, the results showed that these mutants exhibited varying phenotypes under the same growth conditions (Tjita, 2021; Hong, 2023). As a result, guided by the method proposed by Nishihama et al. (2018), we performed the gene editing via thallus transformation – essentially, tissue culture using the CRISPR-Cas9 technique.

Tudor Staphylococcal Nuclease (TSN) is a protein conserved in eukaryotes with the exception of *Saccharomyces cerevisiae* (Frei dit Frey et al., 2010; Gutierrez-Beltran et al., 2015; Gutierrez-Beltran et al., 2016). In animals, it is known that TSN interacts with several component of RISC complex, for example, AGO1(Gutierrez-Beltran et al., 2016). Our previous study concerning in *P1/HC-Pro*^{Tu} plant, P1 interacts with TSN1 and TSN2 (Hu et al., 2020). P1 protein has been shown to be very important, as it can enhance the function of HC-Pro. Previous study has shown that TSN is related to stress response in Arabidopsis and is indispensable in normal development (Frei dit Frey et al., 2010; Gutierrez-Beltran et al., 2015). We have generated a plant with TSN1 and TSN2 double mutant (*tsn1tsn2*^{ge} mutant) using CRISPR-Cas9 technique, we aim to explore the relationship between TSN and AGO1 in Arabidopsis.

In Arabidopsis, *CURLY LEAF* gene (*CLF*) plays a crucial role in leaf development, flowering, and growth (Singkaravanit-Ogawa et al., 2021). As a member of the polycomb-group genes, CLF serves as the histone methyltransferase of the Polycomb Repressive Complex 2 (PRC2). It is responsible for the trimethylation of lysine 27 on histone H3 (H3K27me3), allowing it to regulate the expression of target genes through H3K27me3 (Kim et al., 1998; Liu et al., 2016; Re et al., 2020; Singkaravanit-Ogawa et al., 2021). Previous study shown that CLF can regulate miRNA activity by controlling the stability of AGO1 protein (Re et al., 2020). Moreover, the Like Heterochromatin Protein1 (LHP1), also known as Terminal Flower 2 (TFL2), is a highly evolutionary conserved protein that has been shown to interact with the PRC2 (Derkacheva et al., 2013;

doi:10.6342/NTU202303945

Feng and Lu, 2017). Previous report have also indicated that the AGO1 protein is decreased in *lhp1* mutated line (Re et al., 2020). We created a mutant of CLF (*clf*^{ge} mutant) and LHP1 (*lhp1*^{ge} mutant) using CRISPR-Cas9 technique for testing the AGO1 levels and activity.

Table 1 listed the observations of all mutants performed in this study. The study presented appears to involve the manipulation of various genes in *M. polymorpha* and Arabidopsis using CRISPR-Cas9 technique and an exploration of how these mutations could affect AGO1 levels and activities. The key findings and their implications are as follows: (1) CRISPR-based mutation of Mp*DCL4*, Mp*HYL1*, and *MIR11707* through the thallus transformation obtained the stabilized morphologic phenotype under the same growth conditions, enhancing the reliability of morphological studies compared to the mutants that generated through spooring transformation. (2) The morphological study and evaluation of AGO1 activity were conducted in the *P1/HC-Pro*^{Tu}*/ATG8a*+/+ plants. (3) With interest in the *TSN1* and *TSN2* and their relationship to P1 and AGO1, the *tsn1tsn2*^{ge} mutant was generated. Moreover, the *clf*^{ge} and *lhp1*^{ge} mutants were explored with the AGO1 levels and activities through *in vitro* RISC activity assay. Further investigations with these homozygous mutants will be done to explore the impact of these gene functions on AGO1 stability and activity. Additionally, further investigation is needed to understand the mechanistic underpinnings of the observed changes in AGO1 levels in different mutants.

doi:10.6342/NTU202303945

Materials and methods

Plant materials and growth conditions

Marchantia polymorpha Takaragaike-1 (Tak1, male accession) and *Arabidopsis thaliana* Columbia ecotype (Col-0) were used as wild types. *P1/HC-Pro*^{Tu} (Hu et al., 2020), *P1/HC-Pro*^{Tu}*/atg8a*^{ge} (Wei et al., 2022), and *P1/HC-Pro*^{Tu}*/ATG8a +/+* transgenic plants or mutants were used in this study. *M. polymorpha* gemma and thallus were grown and maintained on half-strength Gamborg's B5 medium containing 1% agar, and MES 2-(N morpholino) ethanesulfonic. *A. thaliana* seeds were surface sterilized before being sown on Murashige and Skoog (MS) medium with/without suitable antibiotics. Seedlings were transferred into BVB substrates, vermiculite and perlite under ratio of 3:1:1 after 10-14 days of germination. All plants were grown at 24°C in a growth room with 16 h of light/8 h of dark unless other specified.

Vector construction and CRISPR/Cas-9-mediated mutations

Guide RNA (gRNA) sequences were given by our lab seniors as listed in Table 2. Two gRNAs were cloned into pMpGE010 binary vector to create pMpGE010-DCL4, pMpGE010-HYL1, pMpGE010-miR11707 plasmids. Thallus from *M. polymorpha* Tak-1 accession was cut and cultured on half-strength Gamborg's B5 medium containing 1% sucrose, 1% agar and MES 2-(N morpholino) ethanesulfonic for three days. The plasmids were then transformed into agrobacteria GV2260 strain for incubation and introduced into *M. polymorpha* thalli by culturing agrobacteria with thallus in 0M51C medium with 100 μM acetosyringone and co-cultivated at 22°C with agitation at 130 r.p.m. for 48 h (Ishizaki et al., 2008). Thalli were then collected and selected on plates containing 12.5 μg/mL hygromycin B and 100 μg/mL cefotaxime.

doi:10.6342/NTU202303945

Gene editing for Arabidopsis with CRISPR-Cas9

Guide RNA (gRNA) was designed according to the protospacer adjacent motif (PAM) found on *TSN1*, *TSN2*, *CLF*, and *LHP1* genomic regions. Guide RNAs for each gene as indicated in Table 2 were cloned into pHEE401E binary vector to create pHEE401E-TSN1, pHEE401E-TSN2, pHEE401E-CLF, and pHEE401E-LHP1 plasmids. These plasmids were transformed into *Agrobacterium tumefacien* GV3101 strain for floral dipping with Col-0 plant through procedure stated by Clough and Bent (1998). Murashige and Skoog (MS) medium with 15 μg/mL Hygromycin B was used as selective plates for transformants screening.

Genotyping

For detection of mutation generated by CRISPR/Cas-9, genomic DNA was extracted from 10 mg thalli of Mp*dcl4*^{ge}, Mp*hyl1*^{ge}, Mp*miR11707*^{ge} or 10 mg leaves of *P1/Hc-Pro*^{Tu}/ATG8a +/+, At*clf*^{ge}, At*lhp1*^{ge}, At*tsn1tsn2*^{ge}, using 100 μl DNA extraction buffer (100 mM Tris-HCl, pH 9.5, 1 M KCl, 10 mM EDTA). Extracted DNAs were then mixed with specific forward and reverse primers (as listed in Table 3), Taq DNA polymerase 2x Master Mix RED (Ampliqon) and proceed with PCR amplification. After amplification, the PCR products were checked by electrophoresis at 130 volt for 20 min. Some of the PCR products were cleaned up by Exo-SAP reaction (Exonuclease I, 10× Exo I buffer, Shrimp Alkaline Phosphate SAP, 10× TAE buffer) and sent for sequencing for mutant determination. Vector NTI, AlignX and ContigExpress software were used to compare the mutant sequence to the reference, and mutation data were collected.

doi:10.6342/NTU202303945

Western blot analysis

14-day-old of plant seedlings were homogenized with 1× PBS and denatured in 2x SDS sample buffer (4% SDS, 20% glycerol, 1% β-mercaptoethanol, 0.01% bromophenol blue, 0.1 M Tris-HCl, pH 6.8). After incubation at 100ºC for 10 min, samples were ready to be tested or can be stored at -20ºC. For Western blot analysis, samples were analysed on 7.5% and 10% SDS polyacrylamide gel by electrophoresis. The separated proteins were then transferred to a PVDF membrane (GE healthcare) with transfer buffer (50 mM Tris base, 40 mM glycine, 1 mM SDS, and 20% methanol) by electroblotting. Followed by blocking with 7% skim milk in wash buffer (25 mM Tris-HCl, pH 7.5, 150 mM NaCl, 0.1% Tween-20) and incubation with appropriate antibodies in 5% skim milk. Primary antibodies that were used are polyclonal antibodies at specific dilutions, whereas for secondary antibody, HRP-conjugated anti-rabbit IgG (10,000× dilution) (GE healthcare) were used. Immuno-stained proteins were developed with the WesternBright ECL system and the signal was visualized by chemiluminescence detection with a Western Lightning™ Pro kit (PerkinElmer). Polyclonal Actin antibody (5,000× dilution; Agrisera, AS13 2640) was used for control. The signal was visualized by enhance chemiluminescence detection with Western Lighting™ Pro kit (PerkinElmer). The signal for each protein was detected using ImageJ and was normalized with wild type signal, which was detected by ImageJ.

AGO1-IP and *in vitro* RISC assay

cDNA fragment, *MYB33*-230 (Hong et al., 2023), containing miRNA target site, was amplified with the specific primer set and cloned into a pGEM-T easy vector (Promega). The DNA template for *in vitro* transcription was amplified. RNA was

doi:10.6342/NTU202303945

synthesized using the Promega Transcription Kit (Riboprobe System-T7, Promega, P1440) with the DNA template and the addition of 1 μL fresh [α-P32] UTP (PerkinElmer). Unincorporated UTP was removed by G50 resin (Cytiva). The RNA transcript was separated on a 6% denaturing PAGE gel in 0.5× TBE buffer (29:1 acrylamide/bis (Bio-Rad), 8 M urea), and the PAGE gel was exposed to chemiluminescence film (Cytiva) to visualize the RNA. The band with a strong signal was excised and mashed in 300 μL extraction buffer (250 mM NaOAC, 1 mM EDTA) and passed through centrifuge tube filters (Costar). The supernatant was further cleaned up using the TRIzol method. RNA was diluted with water to obtain a radioactive strength of 200 to 500 CPM per 5 μL.

For AGO1-IP, 15 μL 1 mg/mL IgG and 30 μL protein A/G beads (Cytiva) were mixed and preincubated for 30 min following the user's manual. Plant tissues (0.5 g) were ground, and the tissue lysate was extracted with 1 mL AGO1-IP buffer (50 mM Tris–HCl pH 7.5, 150 mM NaCl, 5 mM $MgCl_2$, 0.1% Nonidet P-40, and 10% glycerol, 1× Protein inhibitor, 5 mM DTT). The tissue lysate was centrifuged at 8,000 rpm for 5 min, and the supernatant was mixed with IgG beads after filtered with a 0.45 μM filter. The reaction was incubated at 4°C for 2 h under rotation. The AGO1 precipitates were then washed four times with IP buffer and mixed with 1× PBS buffer. The IP products were further used for small RNA extraction, western blotting, or in vitro RISC assay and the presence of AGO1 in the IP product was quantified based on the standard recombinant AGO1-N protein by western blotting with the α-AGO1 antibody.

For the slicer assay, 5 μL 32P-labeled substrate RNA (200-500 CPM/ 5 μL) in 25 μL 2× cleavage buffer [2× PBS, 266.6 mM KCl, 26.6 mM $MgCl_2$, 33.4 mM DTT, 6.6 mM ATP, 1.4 mM GTP, 0.25% RiboLock (Thermo Scientific)] incubated with AGO1-IP beads at 25°C for 1.5 h under rotation. The RNA fragment was purified with the TRIzol

doi:10.6342/NTU202303945

method. The RNA was solubilized in 10 μL water with 10 μL RNA Gel Loading Dye (Invitrogen) and denatured at 80°C for 5 min. The RNA was separated on 6% denaturing PAGE gel and exposed to chemiluminescence film to obtain the image.

doi:10.6342/NTU202303945

Result

CRISPR-Cas9 mediated *M. polymorpha* HYL1 mutation

HYL1 is a double stranded RNA binding protein which known involved in the miRNA biogenesis in plant(Lu and Fedoroff, 2000; Han et al., 2004; Vazquez et al., 2004; Dong et al., 2008; Tjita, 2021). To the interest of this protein in *M. polymorpha*, we performed mutation on *M. polymorpha* through CRISPR-Cas-9. Two gRNAs, HYL1-gRNA1 (9,659,158 bp, chromosome 7) and HYL1-gRNA2 (9,659,244 bp, chromosome 7) (Table 2), which both located at a different site of exon 2 on Mp*HYL1* genome, were designed based on the PAM site on Mp*HYL1* genome sequence (Fig. 1A), resulting in 3 individuals of Mp*hyl1*^{ge} mutant lines (line #1-1, #1-5, and #2-4) were obtained (Fig. 1B, C).

The sequencing results revealed each mutant line's insertion and deletion (INDELs) (Fig. 2B, C). In mutant lines created from MpHYL1-gRNA1 editing, Mp*hyl1*^{ge} line #1-1 having 13 basepair (bp) deletion and 44 bp insertion (3n+2 frameshift mutation), Mp*hyl1*^{ge} line #1-5 having 3 bp insertion (in frame mutation) whereas in mutant line created from MpHYL1-gRNA2 editing, Mp*hyl1*^{ge} line #2-4 is having 1 bp of Adenine (A) insertion (3n+1 frameshift mutation) (Fig. 1B, C).

Having MpHYL1 sequence in Tak-1 as reference, the amino acid sequences of each mutant line were analysed using Vector NTI and as shown in Figure 2A and B. Mutation with 1 frameshift was indicated as 3n+1, without frameshift as 3n (Fig. 2A, B). By a-MpHYL1 antibody created previously by our lab (Tjita, 2021), MpHYL1 protein was detected by using western blot analysis; however, while the mutated protein sizes were expected as 24.97 kDa in Mp*hyl1*^{ge} line #1-1, 39.05 kDa in Mp*hyl1*^{ge} line #1-5, and 27.5 kDa in Mp*hyl1*^{ge} line #2-4, the protein sizes detected by western blot was higher than expected in Mp*hyl1*^{ge} line #1-1, lower and an extra band was found in Mp*hyl1*^{ge} line #1-

doi:10.6342/NTU202303945

5 and no protein was detected in Mp*hyl1*^{ge} line #2-4 (Fig. 2C). It suggested that MpHYL1 protein (37.3 kDa) were successfully mutated from each of the mutants; however the protein sizes were not same as our prediction by calculating through the amino acid sequence.

For the phenotype of mutants observation, no noticeable morphologic difference between Tak-1 under 22°C (Fig. 3A). Nonetheless, when Mp*hyl1*^{ge} line #1-1 was being grown under far-red light, it was seen that there is only two sexual organs was produced from a gemma, whereas four sexual organs were generated in Tak-1 (Fig. 3B), indicating that MpHYL1 might involve in sexual organ development. In our previous study, *M. polymorpha* has different phenotypes when growing in high temperature (28°C) and normal growth condition (22°C) (Hong, 2023). Therefore, these Mp*hly1*^{ge} mutants were grown in 22°C and 28°C to study their phenotype changes (Fig. 4A & B). Results showed that under 22°C, Mp*hyl1*^{ge} had more rhizoid compared with Tak-1 at 14-day-old. (Fig. 4A). Whereas under 28°C, the thallus of mutant lines showed curled thallus phenotype and significantly denser rhizoid compared to Tak-1 (Fig. 4B), interestingly Mp*hyl1*^{ge} line #2-4 was considerably smaller, and thallus showed more severely curled compared to Tak-1 and other mutant lines, suggesting the effects of temperature on thallus and rhizoid formation of mutant.

CRISPR-Cas9 mediated *M. polymorpha* DCL4 mutation

DCL4 is known to be a dicer protein found in plants that can cleave long dsRNA and produce 21-nt tasiRNA (Parent et al., 2015; Fukudome and Fukuhara, 2017). There are studies related to the function and role of DCL4 in *M. polymorpha* (Mp*DCL4*), but there is a lack of genetic and biochemical analysis of MpDCL4 (Lin and Bowman, 2018).

doi:10.6342/NTU202303945

Thus, in this study, mutation on Mp*DCL4* was done on Tak-1 accession using the CRISPR-Cas9 technique. Two gRNAs, DCL4-gRNA1 (13,047,138 bp on chromosome 7) and DCL4-gRNA2 (13,048,076 bp on chromosome 7), were designed based on the PAM site on Mp*DCL4* genome sequence to perform mutation on *M. polymorpha* (Fig. 5A). One Mp*dcl4*^{ge} mutant lines (line #2-3) was obtained from DCL4-gRNA2 editing with 5 bp insertion (3n+2 frameshift mutation) on exon 6 of Mp*DCL4* genome sequence (Fig. 5B, C). While referring to the Tak-1 *DCL4* sequence, a stop codon was found in the mutant line (Fig. 5D), and thus, MpDCL4 was expected to be mutated in Mp*dcl4*^{ge} line #2-3.

As for the phenotype of mutant lines obtained, there is no obvious difference shown compared with the wild type Tak-1 under 22°C (Fig. 6A). Our previous study suggested phenotypic changes on *M. polymorpha* under high temperature. Therefore, a temperature dependence (22°C and 28°C) phenotype was observed (Fig. 6B & C). The results indicated a curled thallus phenotype and denser rhizoid on Mp*dcl4*^{ge} line #2-3 compared with Tak-1 at 28°C (Fig. 6C), whereas slightly denser rhizoid was observed in Mp*dcl4*^{ge} line #2-3 under 22°C (Fig. 6B). This suggested that phenotype of Mp*dcl4*^{ge} line #2-3 is being more severe under 28°C.

CRISPR-Cas9 mediated *M. polymorpha MIR11707* mutation

Our previous study showed that *MIR11707* is the miRNA that is responsible on regulating AGO1 activity in *M. polymorpha* (Lin et al., 2016). Having an interest in the regulation between *MIR11707* and MpAGO1, we performed mutation of *MIR11707* on *M. polymorpha* Tak-1 accession through the CRISPR-Cas9 technique. Two gRNAs, MIR11707-gRNA1 (2,614,474 bp on chromosome 3) and MIR11707-gRNA2 (2,614,546

doi:10.6342/NTU202303945

bp on chromosome 3), were designed based on the PAM site on Mp*MIR11707* genome sequence (Fig. 7A).

From the sequencing result, five individuals of Mp*mir11707*^{ge} mutant lines (line #1-1, #1-3, #1-6, #2-28, and #2-24) were obtained after CRISPR-Cas9 mutation (Fig. 7B, panel i, ii). Where Mp*mir11707*^{ge} line #1-1, #1-3, and #1-6 are mutation targeting MIR11707-gRNA1 (Fig. 7B, panel i), and Mp*mir11707*^{ge} line #2-28 and #2-24 are mutation targeting MIR11707-gRNA2 (Fig. 7B, panel ii). The sequencing results revealed the insertion and deletion (INDELs) of each mutant line (Fig. 7B), showed Mp*mir11707*^{ge} line #1-1 has 6 bp deletion on *MIR11707.2*, Mp*mir11707*^{ge} line #1-3 has 25 bp deletion with 1 bp of guanine replaced by cytosine and 1 bp of thymine (T) replaced by guanine (G), Mp*mir11707*^{ge} line #1-6 is having 4 bp deletion, Mp*mir11707*^{ge} line #2-28 having 1 bp of thymine (T) insertion, Mp*mir11707*^{ge} line having 1 bp of cytosine (C) deletion (Fig. 7B, panel i, ii).

Having Mp*MIR11707* sequence in Tak-1 as reference, the precursor of each mutants were analysed with Vienna RNAfolding and as shown in Figure 8C. There is no significant change in the structure of the precursor in Mp*mir11707*^{ge} line #1-1, #1-6, #2-24, and #2-28, whereas in the precursor of Mp*mir11707*^{ge} line #1-3, an additional branch loop was found on *MIR11707.1* site, suggesting a succeeded mutation on Mp*MIR11707.1*.

In a previous study, the result suggested phenotypic changes of *M. polymorpha* under different temperatures (Hong, 2023). Thus, we grow the mutants under high (28°C) and normal temperatures (22°C). There is no significant changes in phenotype under 22°C in all Mp*mir11707*^{ge} lines (Fig. 8A), however under 28°C, all of the Mp*mir11707*^{ge} lines showed a more severe curled thallus and the thallus were showed more transparent when

doi:10.6342/NTU202303945

compared to Tak-1 (Fig. 8B), suggesting a phenotype shift of Mp*mir11707*^{ge} lines under high temperature (28°C).

AGO1 studies on *P1/HC-Pro*^{Tu} transgenic lines.

In our previous study, the P1/HC-Pro^{Tu} was indicated with the ability to effect the AGO1 degradation in Arabidopsis (Hu et al., 2020), also in our previous study (Hu et al., 2020; Wei et al., 2022; Ying, 2022) showing that AGO1 protein is significantly downregulated in *P1/HC-Pro*^{Tu} plants. In our previous research, we mutated autophagy *atg8a* in *P1/HC-Pro*^{Tu} plant with CRISPR-Cas9 technique and the AGO1 in *P1/HC-Pro*^{Tu}*/atg8a*^{ge} line showed upregulated compared to *P1/HC-Pro*^{Tu} line, suggested that autophagy is responsible on the AGO1 degradation responding to *P1/HC-Pro*^{Tu} (Wei et al., 2022).

For further study, we crossed the *P1/HC-Pro*^{Tu}*/atg8a*^{ge} line with wild type Col-0 plant to recover ATG8a activity in plant. Genotyping and sequencing were performed for each transgenic line. Three sets of primers were designed to discover the *P1/HC-Pro*^{Tu} and *atg8a* homozygous line, including primer for detecting *ATG8a* sequence, primer for detecting wild type *P1/HC-Pro*^{Tu} T-DNA insertion site, and primer for detecting *P1/HC-Pro*^{Tu} T-DNA (Fig. 9A). As shown in Figure 9A upper panel, *atg8a* was positively detected in *P1/HC-Pro*^{Tu}*/ATG8a* +/+ line #3-1 and #3-2, similar to Col-0 plant and *P1/HC-Pro*^{Tu} plant (positive control) whereas it was negatively detected in *P1/HC-Pro*^{Tu}*/atg8a*^{ge} plant (negative control). At the same time, at middle and lower panel, homozygous *P1/HC-Pro*^{Tu} was positively detected in *P1/HC-Pro*^{Tu}*/ATG8a* +/+ line #3-1 and #3-2, similar to *P1/HC-Pro*^{Tu} and *P1/HC-Pro*^{Tu}*/atg8a*^{ge} plant (positive control), whereas in Col-0 plant, it is detected only in middle panel, which is detecting with primer

doi:10.6342/NTU202303945

targeting wild type *P1/HC-Pro*^{Tu} T-DNA insertion site, indicating that other than Col-0, all samples were having *P1/HC-Pro*^{Tu} T-DNA insertion (Fig. 9A). This suggested that *P1/HC-Pro*^{Tu}*/ATG8a* +/+ line #3-1 and line #3-2 were having homozygous *P1/HC-Pro*^{Tu} and *atg8a* sequence which is our expectation.

The phenotype of 10-day-old *P1/HC-Pro*^{Tu} seedlings was shown in Figure 9B. The length of the cotyledons is indicated as "a", whereas the width of the leaf is marked as "b". The ratio of a:b for cotyledons in various plants was calculated (n=4) (Fig. 9B, panel i). In Col-0 plants, the average ratio was 0.88, whereas the ratio of *P1/HC-Pro*^{Tu} plants was approximately 0.56, indicating a narrower and longer cotyledon (b > a) (Fig. 9B, panel i). Nonetheless, the a:b ratio of *P1/HC-Pro*^{Tu}*/atg8a*^{ge} plants showed an average of 0.68, closer to that of the Col-0 plant (Fig. 9B, panel i), suggesting that the narrow cotyledon phenotype in the *P1/HC- Pro*^{Tu} background was partially recovered in *atg8a* mutants. At the same time, in the *P1/HC-Pro*^{Tu}*/atg8a*^{ge} with ATG8a recovered line (*P1/HC-Pro*^{Tu}*/ATG8a* +/+), the average a:b ratio of *P1/HC-Pro*^{Tu}*/ATG8a* +/+ line #3-1 and #3-2 was 0.54 and 0.62, respectively, indicating that the narrow cotyledon phenotype was restored close to *P1/HC-Pro*^{Tu} plants (Fig. 9B, panel i). Nonetheless, when plants are at 21-day-old, the phenotype occurred as serrated leaves in *P1/HC-Pro*^{Tu} plants as well as *P1/HC-Pro*^{Tu}*/atg8a*^{ge} plant and *P1/HC-Pro*^{Tu}*/ATG8a* +/+ line #3-1 and #3-2, as indicated by arrows in figure 9B, panel ii.

With the presence of HC-Pro protein in all samples except Col-0 (negative control), the signal of AGO1 in *P1/HC-Pro*^{Tu}*/ATG8a* +/+ line #3-2 plant is slightly reduced (0.80- and 0.74-fold) compared to the *P1/HC-Pro*^{Tu}*/atg*8a^{ge} line (1.00- and 0.84-fold), and AGO1 shown recovered comparing *P1/HC-Pro*^{Tu}*/ATG8a* +/+ line #3-2 plant (0.80- and 0.74-fold) to *P1/HC-Pro*^{Tu} plant (0.54- and 0.62-fold) (Fig. 10A, upper panel). Col-0 as positive control, AGO1 signal is similar to *P1/HC-Pro*^{Tu}*/atg8a*^{ge} line (Fig. 10A).

doi:10.6342/NTU202303945

Next, the activity of AGO1 as a RISC component in each of the transgenic lines, that is Col-0 plant (positive control), *P1/HC-Pro*^{Tu} plant, *P1/HC-Pro*^{Tu}*/atg8a*^{ge}, and *P1/HC-Pro*^{Tu}*/ATG8a* +/+ line #3-2, was tested by performing *in vitro* RISC activity assay. In our previous study, RNA substrate *MYB33* (*MYB33-230*) proved cleaved by AGO with the regulation of *MIR159* in Col-0 plant (Hong et al., 2023). Result showed a successful cleavage on Col-0, *P1/HC-Pro*^{Tu} plant, *P1/HC-Pro*^{Tu}*/atg8a*^{ge}, and *P1/HC-Pro*^{Tu}*/ATG8a* +/+ mutant line #3-2 with signals at 5′ and 3′ region was showed as arrow (Fig. 10B, panel i). Figure 10B, panel ii showed the presence of AGO1 in all samples. In summary, when the HC-Pro^{Tu} protein level is higher in plants, AGO1 level is downregulated simultaneously. Western blot analysis on all the transgenic lines showed that atg8a is related to AGO1 degradation. At the same time, the cleavage activity of RISC is shown with the presence of AGO1.

AGO1 studies on *tsn1tsn2*^{ge} transgenic lines.

In the interest of this interaction between P1 and TSN1/2, our lab developed a *tsn1tsn2*^{ge} mutant line with the background of the Col-0 ecotype. Genotyping and sequencing was performed to confirm the mutation of each line. As indicated in Figure 11A panels i and ii, three primers were designed to determine the mutants, which include TSN1-P1M1 and TSN1-P1M3 for *TSN1* genotyping and TSN2-P1M1 primer set for *TSN2* genotyping. In Figure 11B, the result shows that only one mutant line, t*sn1tsn2*^{ge} line #2-2, was found to be mutated with both *TSN1* and *TSN2* genome, whereas two lines (line #6-2, #6-3) showed mutation on *TSN1* only and one line (line #8-5) showed mutation on *TSN2* only (Fig. 11B). At the same time, the phenotype of *tsn1tsn2*^{ge} at 22-day-old was observed, and it showed an average of 1.17-fold longer petiole than in Col-0 (Fig. 11C).

doi:10.6342/NTU202303945

The *tsn1tsn2*^{ge} line #2-2 was then sent for sequencing, and the result showed the editing of the mutant compared with wild-type Col-0 TSN protein, indicating that there is 978 bp was deleted in TSN2 protein (Fig. 12A) with 3n frameshift. The amino acid sequence prediction showed amino acid deletion without any stop codon found (Fig. 12B).

Next, the function of AGO1 in the mutant line was investigated. The western blot analysis on the level of AGO1 in *tsn1tsn2*^{ge} was analysed. The result showed that the AGO1 level of the *tsn1tsn2*^{ge} line #2-2 was upregulated in 2.14- and 2.69-fold compared with wild-type Col-0 (Fig. 13A). We also performed *in vitro* RISC activity assay with RNA substrate *MYB33-230* which regulated by *MIR156* (Fig. 13B, panel ii). Cleavage activity was observed in both Col-0 and *tsn1tsn2*^{ge} line #2-2 with the signal of 5' and 3' region of RNA substrate detected (as indicated as arrows, Fig. 13B, panel i). Western blot analysis result in figure 13B, panel ii showed the presence of AGO1 in all samples, suggesting the involvement of AGO1 in the cleavage of all samples.

AGO1 studies on *clf*^{ge} transgenic lines.

Previous study revealed that CLF is involved in the regulation of AGO1 degradation (Re et al., 2020). We further studied this phenomenon by generating *clf*^{ge} mutant through the CRISPR-Cas9 technique. Genotyping was done to confirm the mutation on each line. Two sets of primers were designed to detect mutation in three different gRNAs, which are located in different sites of the *CLF* genome, including CLF-P1M1 for CLF-gRNA1 genotyping and CLF-P2M2 for CLF-gRNA3 and CLF-gRNA5 genotyping (as indicated in Fig. 14A). The results showed that one mutant line *clf*^{ge} line #4-4 is having possibilities to have homozygous mutated *CLF* as the signal showed deletion in *CLF* gene in CLF-P1M1 compared with Col-0 plant (Fig. 14B). Phenotypic observation was done on 22-

doi:10.6342/NTU202303945

day-old *clf*^{ge} plants and phenotype showed curled leaves (as indicated by arrow), early flowering, and shorten growth stage (leaves are smaller and more than Col-0 at same-day-old) (Fig.14C).

The mutant *clf*^{ge} line #4-4 was sent for sequencing to confirm the deletion of sequence (Fig. 15A). The sequencing results reveal the mutation on mutant line (Fig. 15A), showing that there is 66 bp of deletion in CLF at CLF-gRNA1 site (in-frame mutation, 3n frameshift) (Fig. 15A, panel i), 1 bp of Thymine (T) insertion (3n+2 frameshift) and 1 bp of Guanine (G) insertion (3n+2 frameshift) in CLF-gRNA2 and CLF-gRNA3 site, respectively (Fig. 15A, panel ii, and iii). The amino acid sequence showed no stop codon on the CLF-gRNA1 site (Fig. 15B, panel i), and a stop codon was found on the CLF-gRNA2 site (Fig. 15B, panel ii), suggesting a successful mutation on CLF protein in *clf*^{ge} line #4-4.

To determine the AGO1 activity in each line, western blot analysis was performed using a homemade α-AtAGO1 antibody. Results showed a significantly reduced AGO1 signal (0.38 and 0.14-fold) in the *clf*^{ge} line #4-4 compared with wild type Col-0; slightly reduced in AGO1 level (0.70- and 0.82-fold) was observed in *clf*^{ge} line #4-2 compared with Col-0; and similar AGO1 level (0.99-fold) in *clf*^{ge} line #2-5 compared with Col-0 (Fig 16A, upper panel).

In vitro RISC activity assay was performed with *clf*^{ge} line #4-4 with RNA substrate *MYB33-230* that was regulated by *MIR159* (Fig. 16B). Result showed a successful cleavage of RNA substrate having signals on the 5′ region and 3′ region of RNA substrate detected as indicated by arrow (Fig. 16B, panel i). Western blot analysis showed the presence of AGO1 in all samples, indicating the involvement of AGO1 in the cleavage activity on all samples (Fig. 16B, panel ii).

doi:10.6342/NTU202303945

AGO1 studies on *lhp1*^{ge} transgenic lines.

Previous report has demonstrated that AGO1 was shown to be decreased in the *lhp1* mutated line compared to the Col-0 plant (Re et al., 2020). In the interest of the AGO1 degradation phenomenon, the *lhp1*^{ge} mutant line was produced by our lab. First, genotyping and sequencing were performed to detect the succeeded mutant line (Fig. 17B) with 2 sets of primers, including P1M1 for LHP1-gRNA2 genotyping and LHP1-P2M2 for LHP1-gRNA3 and LHP1-gRNA5 genotyping (as indicated in Fig.17A). Result suggested that *lhp1*^{ge} line #3-3 is having mutation (deletion) on *LHP1* gene at LHP1-P2M2 site (Fig. 17B, lane 5-7) compared to wild type Col-0 plant (Fig. 17B, first and last lane) where the band is showed lower in mutant line than in Col-0. The phenotypic study was done on the 22-day-old plant of *lhp1*^{ge} mutants, and the result showed a very small leaf size and early flowering phenotypes compared with Col-0 plants (Fig. 17C), suggesting a mutation occurred in all lines.

Western blot analysis was performed to detect AGO1 levels on the mutant lines. The results showed that compared with Col-0 (positive control, 1.00- & 1.70-fold), in *lhp1*^{ge} line #1-9, one of the samples (Fig. 18A, lane 3) showed increased (2.39-fold) while another sample (Fig. 18A, lane 4) showed similar level (1.09-fold) compared to Col-0 plants, whereas in *lhp1*^{ge} line #3-3 (Fig. 18A, lane 5 & 6) showed significant upregulated AGO1 level (2.93- and 3.00-fold), and in *lhp1*^{ge} line #3-8 (Fig. 18A, lane 7 & 8), the AGO1 was slightly downregulated (0.70- and 0.83-fold), indicating *lhp1*^{ge} mutant lines had different AGO1 level.

As the genotyping result in Figure 17B showed, *lhp1*^{ge} line #3-3 possibly has a homozygous mutation on the *LHP1* genome. Thus, the activity of AGO1 in the *lhp1*^{ge} line

doi:10.6342/NTU202303945

#3-3 was detected by *in vitro* RISC activity assay with its cleavage activity on RNA substrate *MYB33-230* which was regulated by *MIR159* (Fig. 18B, panel i). The result showed cleavage occurred in both the mutant line and Col-0 (Fig. 18B, panel i) that 5′ region and 3′ region of RNA substrate were detected as indicated by the arrow in Figure 18B, panel i. Western blot analysis showed the AGO1 presence in all samples (Fig. 18B, panel ii), suggesting the involvement of AGO1 in all samples.

doi:10.6342/NTU202303945

Discussion

Mutation of DCL4, HYL1, and *MIR11707* in *M. polymorpha* by thallus transformation produced a more stable phenotype on CRISPR-Cas9 generated mutants.

DCL4 and HYL1 involve in miRNA biogenesis and so are essential components in regulation of post transcriptional gene silencing. Lin et al. (2016) demonstrated that miR11707 regulates Mp*AGO1*; however, the mutation on Mp*AGO1* results the lethal plant (Hong, 2023). Hong (2023) showed the knocked-out *MIR11707* through the spooring transformation by CRISPR-Cas9 gene editing, resulting in the variation of the progenies' phenotypes. Through the thallus transformation, that is, the tissue culture approach on same background as Tak-1 accession, these *mir11707*^{ge} mutants were having identical morphologic phenotype with Tak-1 at 22°C, suggesting that the same of genetic background for the new created mutants can solved the phenotype variations of sporing transformation. The same observations were shown in *dcl4*^{ge} and *hyl1*^{ge} mutants, indicating the potential of tissue culture by CRISPR-Cas9 technique to generate stable mutant for a more reliable morphological study on *M. polymorpha* mutants.

As reported previously, when crossing parental lines with different genetic backgrounds, sporelings are heterogeneous in *M. polymorpha*, and so might affect consistencies among the resulting mutant lines (Kubota et al., 2014). When we mutate *M. polymorpha* with spooring transformation, the genome is edited by meiosis, which may cause mutation not only at gRNAs targeting site but also at another unforeseen site. As we know that *M. polymorpha* is haploid, a single mutation can cause significant effects on the plant development and therefore a slight difference in mutation can cause totally different phenotype in mutants. Thus, when targeting to generate several mutant lines, they will possess with completely different phenotype and cause difficulty in observing

doi:10.6342/NTU202303945

morphological features of plant. While thallus transformation is tissue culture method, the next generation comes from single cell division which involve only mitosis gene editing, therefore the mutation on the genome is more specific and having less possibility of "out of target" mutation. Thus, a more stable phenotype could be expected on different mutant line and so ease the morphological study of mutants.

Increasing of rhizoid phenotype in Mp*hyl1*^{ge} mutant and the mutant lines need further investigation.

HYL1 is a double stranded RNA binding protein which involved in miRNA biogenesis in plant (Vazquez et al., 2004; Tjita, 2021; Wieczorek et al., 2023). In this study, it is shown that Mp*hyl1*^{ge} lines were having obviously more rhizoid under 28°C compared with Tak-1 (Fig. 4B), suggesting HYL1 might have involved in root development of *M. polymorpha* under high temperature. Further studies could be done to confirm the role of HYL1 in rhizoid development and in high temperature.

Nonetheless, in this study after the Mp*hyl1*^{ge} lines was confirmed, western blot analysis was done to confirmed the predicted protein sizes of each mutant which calculated based on the amino acid sequence (Fig. 2C). However, having the expected protein sizes which were 24.97 kDa in Mp*hyl1*^{ge} line #1-1, 39.05 kDa in Mp*hyl1*^{ge} line #1-5, and 27.5 kDa in Mp*hyl1*^{ge} line #2-4, the protein sizes detected are larger than predicted size in Mp*hyl1*^{ge} line #1-1, smaller and an extra band was observed in Mp*hyl1*^{ge} line #1-5. Moreover no detected MpHYL1 in Mp*hyl1*^{ge} line #2-4, which is no march with the mutation prediction (Fig. 2C). On this phenomenon, we think that there might have unexpected mutation (insertion or deletion) on the genome which was not included in the designed primers. Thus, further studies on the sequence of mutant line with whole genome

doi:10.6342/NTU202303945

sequencing is required to confirmed the extra mutation that is out of genotyping detection and to confirm the protein sequence of HYL1. The same studies could be performed on Mp*dcl4*^{ge} and Mp*MIR11707*^{ge} generated in this study.

Unexpected variation between *P1/HC-Pro*^{Tu} and *P1/HC-Pro*^{Tu}*/ATG8a* +/+ transgenic lines could be resulted by unforeseen epigenetic changes.

In our previous study, the phenotypic observation on *P1/HC-Pro*^{Tu} transgenic line was done (Lin et al., 2016). After crossing *P1/HC-Pro*^{Tu}/*atg8a*^{ge} line to Col-0 and producing *P1/HC-Pro*^{Tu}/*ATG8a* +/+ line, it was expected that the phenotype should recovered to a level of *P1/HC-Pro*^{Tu} transgenic line. However, the phenotype of *P1/HC-Pro*^{Tu}/*ATG8a* +/+ plant is showed milder comparing to their parental *P1/HC-Pro*^{Tu} plant (Fig. 9B, panel i, ii). We propose that parental *P1/HC-Pro*^{Tu} plant is the first generation of a transgenic plant and the HC-Pro^{Tu} suppressor may lead to epigenic alterations, such as DNA methylation, at the T-DNA insertion site or the other chromosomes. However, the *P1/HC-Pro*^{Tu}/*ATG8a* +/+ plant, which was produced by crossing with Col-0 plants, likely underwent chromosomal crossover between paternal and maternal chromosomes. This process might have exchanged or altered epigenic markers, resulting in morphologic changes that differ from the parental *P1/HC-Pro*^{Tu} plant. Therefore, morphologic phenotype of *P1/HC-Pro*^{Tu}/*ATG8a* +/+ plant were not identical with parental *P1/HC-Pro*^{Tu} plant, which might also affect the AGO1 levels in the ATG8a complementation lines.

In addition, the *P1/HC-Pro*^{Tu} line did not show a significant reduce in the cleavage activity of AGO1 through *in vitro* RISC activity, which resulted in a conflict to our previous study from Hong et al. (2023). This might due to the variation of the AGO1-IP

doi:10.6342/NTU202303945

when pulling down with the α-AGO1 antibody, resulting in differ concentration of AGO1. Further experiments are needed to ensure these variation.

Further studies on interaction of TSN1 and TSN2 with P1 and AGO1.

TSN as a highly conserved protein in eukaryotes, is known interacting with RISC complex in animal (Gutierrez-Beltran et al., 2016). Being known interacting to P1 in previous study (Hu et al., 2020). In this study, the AGO1 signal in *tsn1*^{ge}/*tsn2*^{ge} is higher signal comparing with Col-0, suggesting that TSN1/2 might involve in AGO1 regulation. Along with the possible regulation to the uncapping of mRNA (Hu et al., 2020), the relation between TSN1, TSN2, P1 and AGO1 will be further studied.

Further studies on LHP1 and CLF in AGO1 activity.

Being known in previous studies, LHP1 can interact with PRC2 (such as CLF) and AGO1 is significantly decreased in *LHP1* and *CLF* mutated Arabidopsis (Derkacheva et al., 2013; Re et al., 2020). Indeed, the AGO1 level was showed unstable in *lhp1*^{ge} mutant in this study (Fig. 18A) line. While observing phenotype in these mutant lines, we found out that there are different severity of phenotypes on individual line, suggesting that these mutant lines might be heterozygous. Therefore, while selecting plant to perform western blot analysis, the heterozygous mutant that we selected might have 50% of normal LHP1 protein, resulting in different AGO1 levels in each samples. Indeed, *lhp1*^{ge} mutant line #1-9, and line #3-3 showed higher AGO1 level, whereas only line #3-8 has slightly reduced in AGO1 levels (Fig. 18A) which might result in affecting the observation of *in vitro* RISC activity in Fig. 18B. The same situation was also observed in *CLF* mutated line, that there is no significant decrease in AGO1 level on mutant line #2-5 and #4-2 (Fig.

doi:10.6342/NTU202303945

16A) and the *in vitro* RISC activity is similar to the level of Col-0. Due to this unforeseen situation, a more precise condition is required when selecting *lhp1*^{ge} and *clf*^{ge} mutant plants.

In vitro RISC activity assay is a good technique to study AGO1 activity in different mutants.

There is two main pathway related to miRNA, including miRNA biogenesis pathway which one of the related regulating component as HYL1, and miRNA regulating pathways which related to function of AGO1. In order to study each of the pathway, there had been few approaches that have been using up until now. For miRNA biogenesis pathway, northern blot analysis has been known to be able to study the different miRNA level. However for miRNA regulation pathway, other than observing the final substrate, there is no direct observing method to study the cleavage activity. Our previous study by Hong et al. (2023) demonstrated that *in vitro* RISC activity assay as a method to study the cleavage efficiency of different transgenic lines. Although in this study, the cleavage activity of different mutant lines is not having significant difference, it is still a handy attempt to study the activity of AGO1. Despite of the *in vivo* study could have a more factual study on living organism, it is having limitations on targeting particularly in the role and function of different component involved in pathways. On the contrary, *in vitro* RISC activity assay is having higher potential to study the regulation of different pathway by pulling down specific protein of interest and observe different steps separately. Therefore, *in vitro* RISC activity assay is a very practical method to study components that involved in the cleavage activity related to RISC complex.

doi:10.6342/NTU202303945

Conclusion

In our previous study of mutation on *M. polymorpha*, the mutation was done with the spooring method and the phenotype showed instability along mutant and generations (Lin et al., 2016; Tjita, 2021), which effecting the reliability of morphological study on each mutant. However, in this study, mutants produced through CRISPR-Cas9 established a more stable phenotype, which could be a more reliable method to perform mutation on *M. polymorpha*. This study has demonstrated that by combining CRISPR-Cas9 with T-DNA insertion method, we can perform various of experiment to study relation and function of different protein and even different gene.

By *in vitro* RISC activity assay, we studied each transgenic or mutant line's cleavage activity of RISC complex. This study has demonstrated that, *in vitro* RISC activity assay is a beneficial attempt to explore the miRNA regulation pathway, targeting the study on AGO1 cleavage activity. At the same time, with western blot analysis done on each transgenic lines, we know that the AGO1 levels are indeed affected in all of the transgenic line. Although more precise condition for selecting a mutant is required, results showed significant changes in AGO1 levels in all mutant and transgenic line, suggesting further study could be done to understand the regulation of different mutant on AGO1.

doi:10.6342/NTU202303945

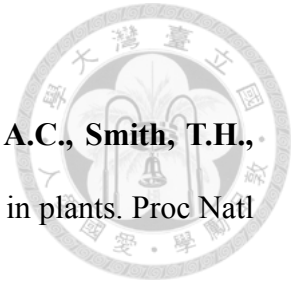

References

Anandalakshmi, R., Pruss, G.J., Ge, X., Marathe, R., Mallory, A.C., Smith, T.H., and Vance, V.B. (1998). A viral suppressor of gene silencing in plants. Proc Natl Acad Sci U S A **95,** 13079-13084.

Anders Hafrén, S.Ü., Anton Hochmuth, Steingrim Svenning, Terje Johansen, Daniel Hofius (2018). Turnip Mosaic Virus Counteracts Selective Autophagy of the Viral Silencing Suppressor HCpro.

Barman, A., Deb, B., and Chakraborty, S. (2020). A glance at genome editing with CRISPR-Cas9 technology. Curr Genet **66,** 447-462.

Berruezo, F., de Souza, F.S.J., Picca, P.I., Nemirovsky, S.I., Martinez-Tosar, L., Rivero, M., Mentaberry, A.N., and Zelada, A.M. (2016). Sequencing of small RNAs of the fern Pleopeltis minima (Polypodiaceae) offers insight into the evolution of the microRNA repertoire in land plants.

Bowman, J.L., Kohchi, T., Yamato, K.T., Jenkins, J., Shu, S., Ishizaki, K., Yamaoka, S., Nishihama, R., Nakamura, Y., Berger, F., Adam, C., Aki, S.S., Althoff, F., Araki, T., Arteaga-Vazquez, M.A., Balasubrmanian, S., Barry, K., Bauer, D., Boehm, C.R., Briginshaw, L., Caballero-Perez, J., Catarino, B., Chen, F., Chiyoda, S., Chovatia, M., Davies, K.M., Delmans, M., Demura, T., Dierschke, T., Dolan, L., Dorantes-Acosta, A.E., Eklund, D.M., Florent, S.N., Flores-Sandoval, E., Fujiyama, A., Fukuzawa, H., Galik, B., Grimanelli, D., Grimwood, J., Grossniklaus, U., Hamada, T., Haseloff, J., Hetherington, A.J., Higo, A., Hirakawa, Y., Hundley, H.N., Ikeda, Y., Inoue, K., Inoue, S.I., Ishida, S., Jia, Q., Kakita, M., Kanazawa, T., Kawai, Y., Kawashima, T., Kennedy, M., Kinose, K., Kinoshita, T., Kohara, Y., Koide, E., Komatsu, K., Kopischke, S., Kubo, M., Kyozuka, J., Lagercrantz, U., Lin, S.S., Lindquist, E., Lipzen,

doi:10.6342/NTU202303945

A.M., Lu, C.W., De Luna, E., Martienssen, R.A., Minamino, N., Mizutani, M., Mizutani, M., Mochizuki, N., Monte, I., Mosher, R., Nagasaki, H., Nakagami, H., Naramoto, S., Nishitani, K., Ohtani, M., Okamoto, T., Okumura, M., Phillips, J., Pollak, B., Reinders, A., Rovekamp, M., Sano, R., Sawa, S., Schmid, M.W., Shirakawa, M., Solano, R., Spunde, A., Suetsugu, N., Sugano, S., Sugiyama, A., Sun, R., Suzuki, Y., Takenaka, M., Takezawa, D., Tomogane, H., Tsuzuki, M., Ueda, T., Umeda, M., Ward, J.M., Watanabe, Y., Yazaki, K., Yokoyama, R., Yoshitake, Y., Yotsui, I., Zachgo, S., and Schmutz, J. (2017). Insights into Land Plant Evolution Garnered from the *Marchantia polymorpha* Genome. Cell **171,** 287-304 e215.

Bu, F., Yang, M., Guo, X., Huang, W., and Chen, L. (2020). Multiple Functions of ATG8 Family Proteins in Plant Autophagy. Front Cell Dev Biol **8,** 466.

Derkacheva, M., Steinbach, Y., Wildhaber, T., Mozgova, I., Mahrez, W., Nanni, P., Bischof, S., Gruissem, W., and Hennig, L. (2013). Arabidopsis MSI1 connects LHP1 to PRC2 complexes. EMBO J **32,** 2073-2085.

Dong, Z., Han, M.H., and Fedoroff, N. (2008). The RNA-binding proteins HYL1 and SE promote accurate in vitro processing of pri-miRNA by DCL1. Proc Natl Acad Sci U S A **105,** 9970-9975.

Feng, J., and Lu, J. (2017). LHP1 Could Act as an Activator and a Repressor of Transcription in Plants. Front Plant Sci **8,** 2041.

Frei dit Frey, N., Muller, P., Jammes, F., Kizis, D., Leung, J., Perrot-Rechenmann, C., and Bianchi, M.W. (2010). The RNA binding protein Tudor-SN is essential for stress tolerance and stabilizes levels of stress-responsive mRNAs encoding secreted proteins in Arabidopsis. Plant Cell **22,** 1575-1591.

doi:10.6342/NTU202303945

Fukudome, A., and Fukuhara, T. (2017). Plant dicer-like proteins: double-stranded RNA-cleaving enzymes for small RNA biogenesis. J Plant Res **130,** 33-44.

Gutierrez-Beltran, E., Moschou, P.N., Smertenko, A.P., and Bozhkov, P.V. (2015). Tudor staphylococcal nuclease links formation of stress granules and processing bodies with mRNA catabolism in Arabidopsis. Plant Cell **27,** 926-943.

Gutierrez-Beltran, E., Denisenko, T.V., Zhivotovsky, B., and Bozhkov, P.V. (2016). Tudor staphylococcal nuclease: biochemistry and functions. Cell Death Differ **23,** 1739-1748.

Han, M.H., Goud, S., Song, L., and Fedoroff, N. (2004). The Arabidopsis double-stranded RNA-binding protein HYL1 plays a role in microRNA-mediated gene regulation. Proc Natl Acad Sci U S A **101,** 1093-1098.

Hong, S.F. (2023). The functional investigation of RNA-induced silencing complex in *Marchantia polymorpha* and Arabidopsis.

Hong, S.F., Fang, R.Y., Wei, W.L., Jirawitchalert, S., Pan, Z.J., Hung, Y.L., Pham, T.H., Chiu, Y.H., Shen, T.L., Huang, C.K., and Lin, S.S. (2023). Development of an assay system for the analysis of host RISC activity in the presence of a potyvirus RNA silencing suppressor, HC-Pro. Virol J **20,** 10.

Hu, S.F., Wei, W.L., Hong, S.F., Fang, R.Y., Wu, H.Y., Lin, P.C., Sanobar, N., Wang, H.P., Sulistio, M., Wu, C.T., Lo, H.F., and Lin, S.S. (2020). Investigation of the effects of P1 on HC-pro-mediated gene silencing suppression through genetics and omics approaches. Bot Stud **61,** 22.

Ishizaki, K., Chiyoda, S., Yamato, K.T., and Kohchi, T. (2008). Agrobacterium-mediated transformation of the haploid liverwort Marchantia polymorpha L., an emerging model for plant biology. Plant Cell Physiol **49,** 1084-1091.

doi:10.6342/NTU202303945

Kasschau, K.D., Xie, Z., Allen, E., Llave, C., Chapman, E.J., Krizan, K.A., and Carrington, J.C. (2003). P1/HC-Pro, a viral suppressor of RNA silencing, interferes with Arabidopsis development and miRNA unction. Dev Cell **4,** 205-217.

Kim, G.T., Tsukaya, H., and Uchimiya, H. (1998). The CURLY LEAF gene controls both division and elongation of cells during the expansion of the leaf blade in Arabidopsis thaliana. Planta **206,** 175-183.

Kubota, A., Ishizaki, K., Hosaka, M., and Kohchi, T. (2014). EfficientAgrobacterium-Mediated Transformation of the LiverwortMarchantia polymorphaUsing Regenerating Thalli. Bioscience, Biotechnology, and Biochemistry **77,** 167-172.

Lin, P.C., Lu, C.W., Shen, B.N., Lee, G.Z., Bowman, J.L., Arteaga-Vazquez, M.A., Liu, L.Y., Hong, S.F., Lo, C.F., Su, G.M., Kohchi, T., Ishizaki, K., Zachgo, S., Althoff, F., Takenaka, M., Yamato, K.T., and Lin, S.S. (2016). Identification of miRNAs and Their Targets in the Liverwort Marchantia polymorpha by Integrating RNA-Seq and Degradome Analyses. Plant Cell Physiol **57,** 339-358.

Lin, S.S., and Bowman, J.L. (2018). MicroRNAs in Marchantia polymorpha. New Phytol **220,** 409-416.

Liu, J., Deng, S., Wang, H., Ye, J., Wu, H.W., Sun, H.X., and Chua, N.H. (2016). CURLY LEAF Regulates Gene Sets Coordinating Seed Size and Lipid Biosynthesis. Plant Physiol **171,** 424-436.

Lu, C., and Fedoroff, N. (2000). A mutation in the Arabidopsis HYL1 gene encoding a dsRNA binding protein affects responses to abscisic acid, auxin, and cytokinin. Plant Cell **12,** 2351-2366.

doi:10.6342/NTU202303945

Parent, J.S., Bouteiller, N., Elmayan, T., and Vaucheret, H. (2015). Respective contributions of Arabidopsis DCL2 and DCL4 to RNA silencing. Plant J **81,** 223-232.

Re, D.A., Cambiagno, D.A., Arce, A.L., Tomassi, A.H., Giustozzi, M., Casati, P., Ariel, F.D., and Manavella, P.A. (2020). CURLY LEAF Regulates MicroRNA Activity by Controlling ARGONAUTE 1 Degradation in Plants. Mol Plant **13,** 72-87.

Singkaravanit-Ogawa, S., Kosaka, A., Kitakura, S., Uchida, K., Nishiuchi, T., Ono, E., Fukunaga, S., and Takano, Y. (2021). Arabidopsis CURLY LEAF functions in leaf immunity against fungal pathogens by concomitantly repressing SEPALLATA3 and activating ORA59. Plant J **108,** 1005-1019.

Sugano, S.S., Nishihama, R., Shirakawa, M., Takagi, J., Matsuda, Y., Ishida, S., Shimada, T., Hara-Nishimura, I., Osakabe, K., and Kohchi, T. (2018). Efficient CRISPR/Cas9-based genome editing and its application to conditional genetic analysis in Marchantia polymorpha. PLoS One **13,** e0205117.

Tjita, V. (2021). Investigation of miRNA biogenesis pathway related genes in *Marchantia polymorpha*.

Vazquez, F., Gasciolli, V., Crete, P., and Vaucheret, H. (2004). The nuclear dsRNA binding protein HYL1 is required for microRNA accumulation and plant development, but not posttranscriptional transgene silencing. Curr Biol **14,** 346-351.

Wei, W.-L., Tran, P.-A., Fang, R.-Y., Pham, T.H., Bowman, J., Hong, S.-F., Pan, Z.-J., Shang, Q.-W., Lin, P.-C., Shen, B.-N., Wu, F.-H., Lin, C.-S., Shen, T.-L., and Lin, S.-S. (2022). The additional unique ability of TuMV HC-Pro in inhibiting HEN1 activity for enhancing the autophagic AGO1 degradation in RNA silencing suppression. Research Square.

doi:10.6342/NTU202303945

Wieczorek, P., Jarmolowski, A., Szweykowska-Kulinska, Z., Kozak, M., and Taube, M. (2023). Solution structure and behaviour of the Arabidopsis thaliana HYL1 protein. Biochim Biophys Acta Gen Subj **1867,** 130376.

Ying, A.C.Z. (2022). Investigation of post-transcriptional gene silencing pathway related genes in *Arabidopsis thaliana*.

doi:10.6342/NTU202303945

Tables

Table 1. Summary on all constructs involved in this study.

	AGO1 activity	Phenotype
Mp*HYL1*	Not tested	Dense rhizoid and curled thallus compared with Tak-1 under 28°C, reduced sexual organ under far-red light compared with Tak-1
Mp*DCL4*	Not tested	Dense rhizoid and curled thallus compared with Tak-1 under 28°C
MpMI*R11707*	Not tested	Transparent thallus and curled thallus compared with Tak-1 under 28°C
P1/HC-Pro^{Tu}	Downregulated, having cleavage activity	Curled and serrated leaves, narrow cotyledons
TSN1/TSN2	Upregulated, having cleavage activity	Long petiole (1.17-fold compared with Col-0)
CLF	Downregulated, having cleavage activity	Curled leaves and early flowering
LHP1	Varied level, having cleavage activity	Significantly small plant with early flowering

doi:10.6342/NTU202303945

Table 2. guide RNA (gRNA) sequences for CRISPR-Cas9 editing.

gRNAs	Sequences (5' to 3')	Location
Mp*HYL1*		
HYL1-gRNA1	AGTCGAGAGACCCACTTGAGG	9,659,158 bp, chromosome 7
HYL1-gRNA2	CTTCAGCCGAGGATAACACGG	9,659,244 bp, chromosome 7
Mp*DCL4*		
DCL4-gRNA1	TATACGGCATTGCCGACCAGG	13,047,138 bp, chromosome 7
DCL4-gRNA2	CAGGTCAGTGAGAAGCCCAGG	13,048,076 bp, chromosome 7
Mp*MIR11707*		
MIR11707-gRNA1	GGCCAGTTCCCATGGATGAGG	2,614,474 bp, chromosome 3
MIR11707-gRNA2	TAAGAATGGCCCGAAGAT	2,614,546 bp, chromosome 3
At*TSN1*		
TSN1-gRNA1	CGGACAAGAACGAGCTCAGC	2,321,984 bp, chromosome 5
At*TSN2*		
TSN2-gRNA1	GCTGAACTCATTATTTCCCG	24,824,730 bp, chromosome 5

doi:10.6342/NTU202303945

TSN2-gRNA2	GTTACGGAAGTACTTGGAGG	24,825,708 bp, chromosome 5
At*LHP1*		
LHP1-gRNA2	GGAAAATTAGTGGAGACGGT	5,827,462 bp, chromosome 5
LHP1-gRNA3	CCTGATCCACTAGACCTAAG	5,828,524 bp, chromosome 5
LHP1-gRNA5	GTTACTCTCATAGGTCTGAT	5,829,192 bp, chromosome 5
At*CLF*		
CLF-gRNA1	TCTTTCAGACTCAGTCCTGG	9,955,091 bp, chromosome 2
CLF-gRNA2	TGGTGTCCTCCTGTAGATGA	9,957,448 bp, chromosome 2
CLF-gRNA3	GCAGAAGAAGACAGAAGCCT	9,957,909 bp, chromosome 2

doi:10.6342/NTU202303945

Table 3. Primers used in this study.

Primer name	Sequence (5′ to 3′)	Location
For Mp*MIR11707*: Wild type (MIR11707-F/MIR11707-R)		
MIR11707-F	TGGTACAAATGGCACACAATG	2,614,175 bp, chromosome 3
MIR11707-R	ACACACGCTGTAAGAGATCGG	2,614,809 bp, chromosome 3
For Mp*DCL4*: gRNA1 (DCL4-g1-F/DCL4-g1-R); gRNA2 (DCL4-g2-F/DCL4-g2-R)		
DCL4-g1-F	ATGTGAACTCCGCACGCTAT	13,046,899 bp, chromosome 7
DCL4-g1-R	AGCTAGTGCTCGATGTGCTG	13,047,390 bp, chromosome 7
DCL4-g2-F	CGATGCTTATGCGTGCTCCT	13,047,784 bp, chromosome 7
DCL4-g2-R	GTTACGTTTATCGACAATGTTTCT	13,048,184 bp, chromosome 7
For Mp*HYL1*: Wild type (HYL1-F/HYL1-R)		
HYL1-F	CTGCCTGTGTACCAATCGAC	9,658,943 bp, chromosome 7
HYL1-R	AAGTGATCGCTTCCACGACG	9,659,352 bp, chromosome 7
For At*TSN1*: Wild type (TSN1-P1/TSN1-M1); (TSN1-P3/TSN1-M3)		
TSN1-P1	CATTCGGTTTACCTCAACATC	2,322,123 bp, chromosome 5

doi:10.6342/NTU202303945

TSN1-M1	CCACTTCCACTACCTAAAGAGAG	2,323,098 bp, chromosome 5
TSN1-P3	GCCACGTTTGTCCTCGATTC	2,321,981 bp, chromosome 5
TSN1-M3	CGTAGTTTGCCCACATTTTAACC	2,323,243 bp, chromosome 5
For At*TSN2*: Wild type (TSN2-P1/TSN2-M1)		
TSN2-P1	GCGGGGACTGCTTAGTAGTT	24,824,297 bp, chromosome 5
TSN2-M1	GGAAGAGGACTTTGGTCGTG	24,826,169 bp, chromosome 5
For At*CLF*: gRNA1 (CLF-P1/CLF-M1); gRNA2 & 3 (CLF-P2/CLF-M2)		
CLF-P1	GAGTACTTGAAAATATTCAAGTTGA	9,956,412 bp, chromosome 2
CLF-M1	GAGAGCTCCCTTCTCAACA	9,957,132 bp, chromosome 2
CLF-P2	TCAAGCAGAGAGCTCCCTTC	9,957,125 bp, chromosome 2
CLF-M2	TGTTGAGATTTTTGGAATGAATAGG	9,958,257 bp, chromosome 2
For At*LHP1*: gRNA2 (LHP1-P1/LHP1-M1); gRNA3 & 5 (LHP1-P2/LHP1-M2)		
LHP1-P1	AAAAAAAAGAGAATCCAAAA	5,827,141 bp, chromosome 5

doi:10.6342/NTU202303945

LHP1-M1	TGAGGTTTTAGGTTTTCTAGGTTTA	5,827,787 bp, chromosome 5
LHP1-P2	GCCAACACATGGGAGCCTTTAGAG	5,828,184 bp, chromosome 5
LHP1-M2	TCCGGGAGGTTTCAGATTGTAATTT	5,829,526 bp, chromosome 5
For *ATG8a*: Wild type (PATG8a_4/MATG8a_4)		
PATG8a_4	AAACAGTTCCGTGTAGGCAA	
MATG8a_4	GCCTTTTGTATAGCTGTGGT	
For *P1/HC-Pro*^{Tu}: Wild type (Ch1LP2/Ch1RP2); T-DNA (pBCoRB2-2/Ch1LP2)		
Ch1LP2	CACACTCCTTAGGTTTTTAAGATAGGGTTC	
Ch1RP2	AGAGCCGTTGTATATATGAGTCGTTCTTAG	
pBCoRB2-2	GGTCATAGCTGTTTCCTGTGTG	

doi:10.6342/NTU202303945

Figures

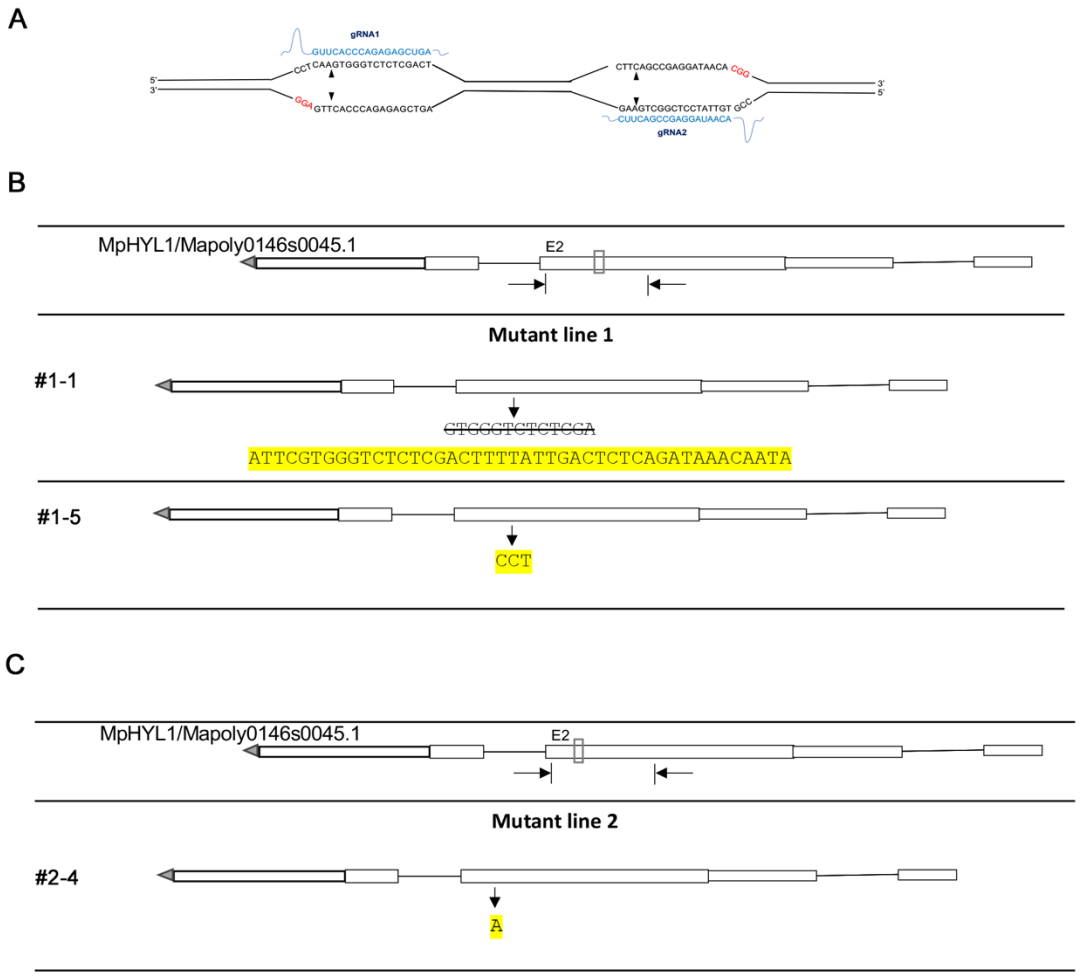

Figure 1. CRISPR-Cas9-mediated mutation on Mp*HYL1*. (A) Two gRNAs were designed for Mp*HYL1* gene editing. Red letters show the Protospacer adjacent motif (PAM) sequence. **(B, C)** Genomic structure of Mp*hyl1*^{ge} mutant lines, with CRISPR-Cas9-introduced INDELs as well as the plant gender of each line. Two small arrows that flank the small box represent forward and reverse primers, whereas the small box shows the gRNA targeted line. Highlighted letters represent insertion, and crossed letters represent deletion.

doi:10.6342/NTU202303945

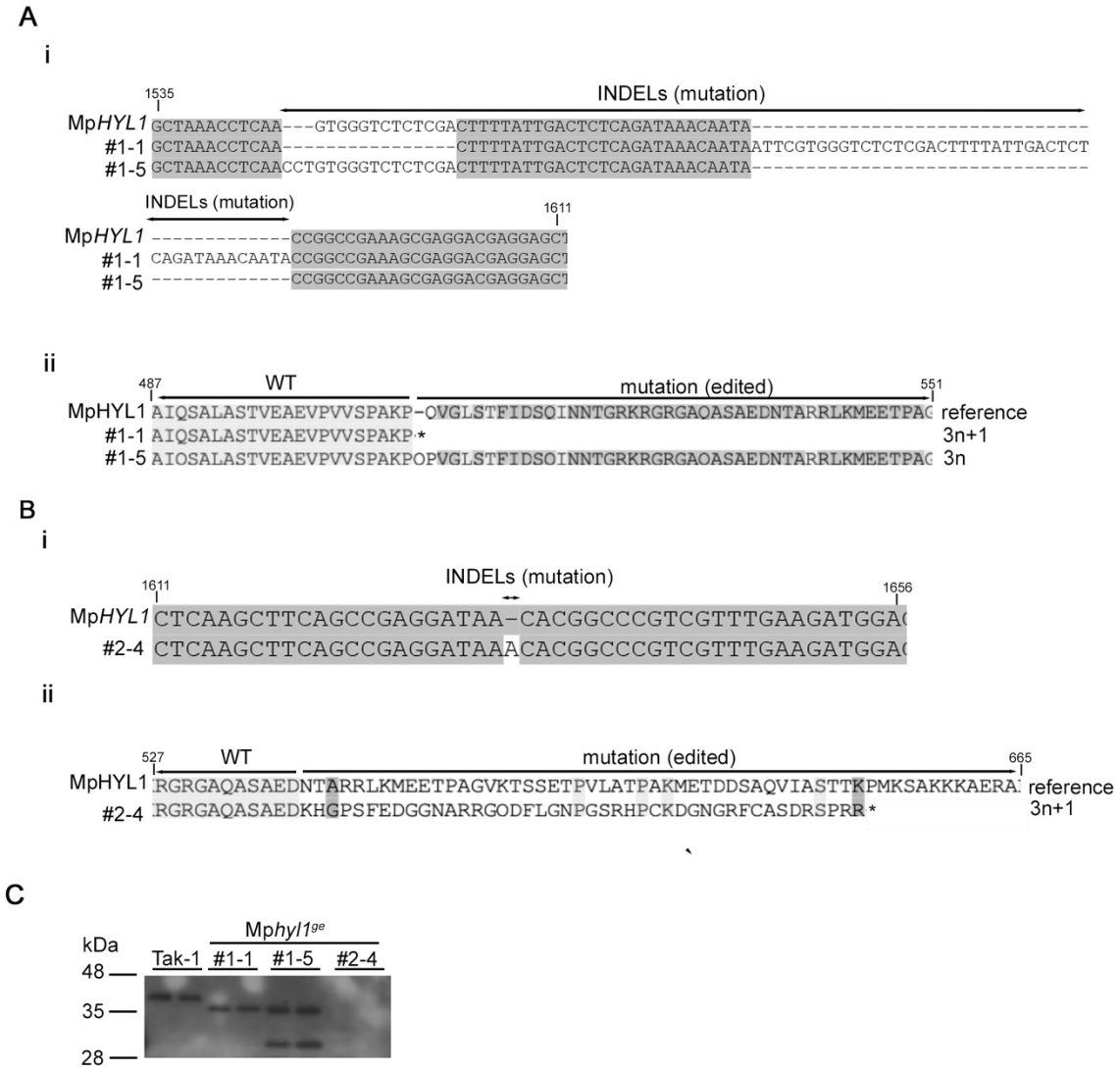

Figure 2. Sequence alignment and protein detection of Mp*hyl1*^{ge} mutants. (A, B) The alignment of the amino acid (i) and nucleotide (ii) sequences with their references on gRNA1 and gRNA2 respectively. Wild type (WT) and mutated site were differentiated by arrows. Box indicates the gRNA editing site. 3n + 1, 3n + 2 reading frames represent the frameshift or asymmetric mutation, whereas 3n indicates symmetric or in-frame mutation. C. Western blot detection of MpHYL1 in each line.

doi:10.6342/NTU202303945

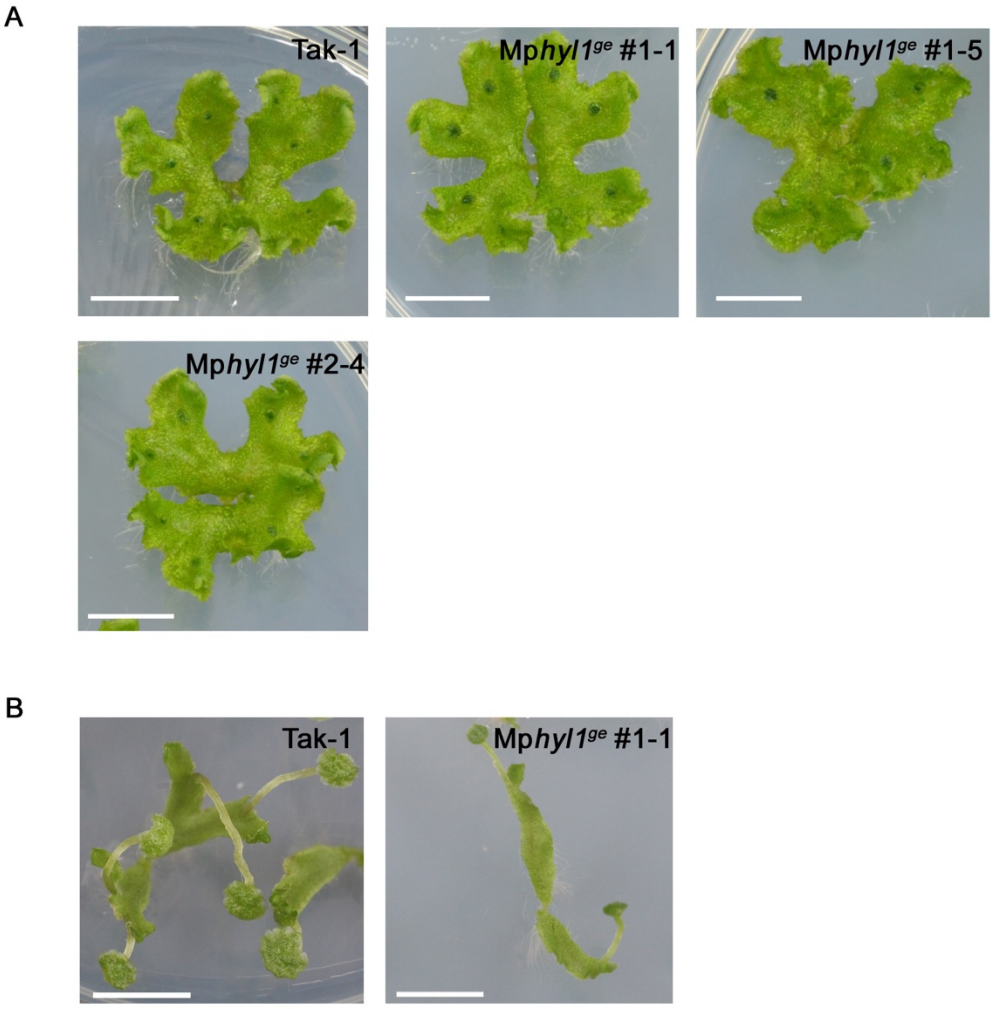

Figure 3. Phenotypic observation of Mp*hyl1*^{ge} mutants. Wild type control: Tak-1. Bars: 1 cm. **A.** under normal growth condition. **B.** under far-red light.

doi:10.6342/NTU202303945

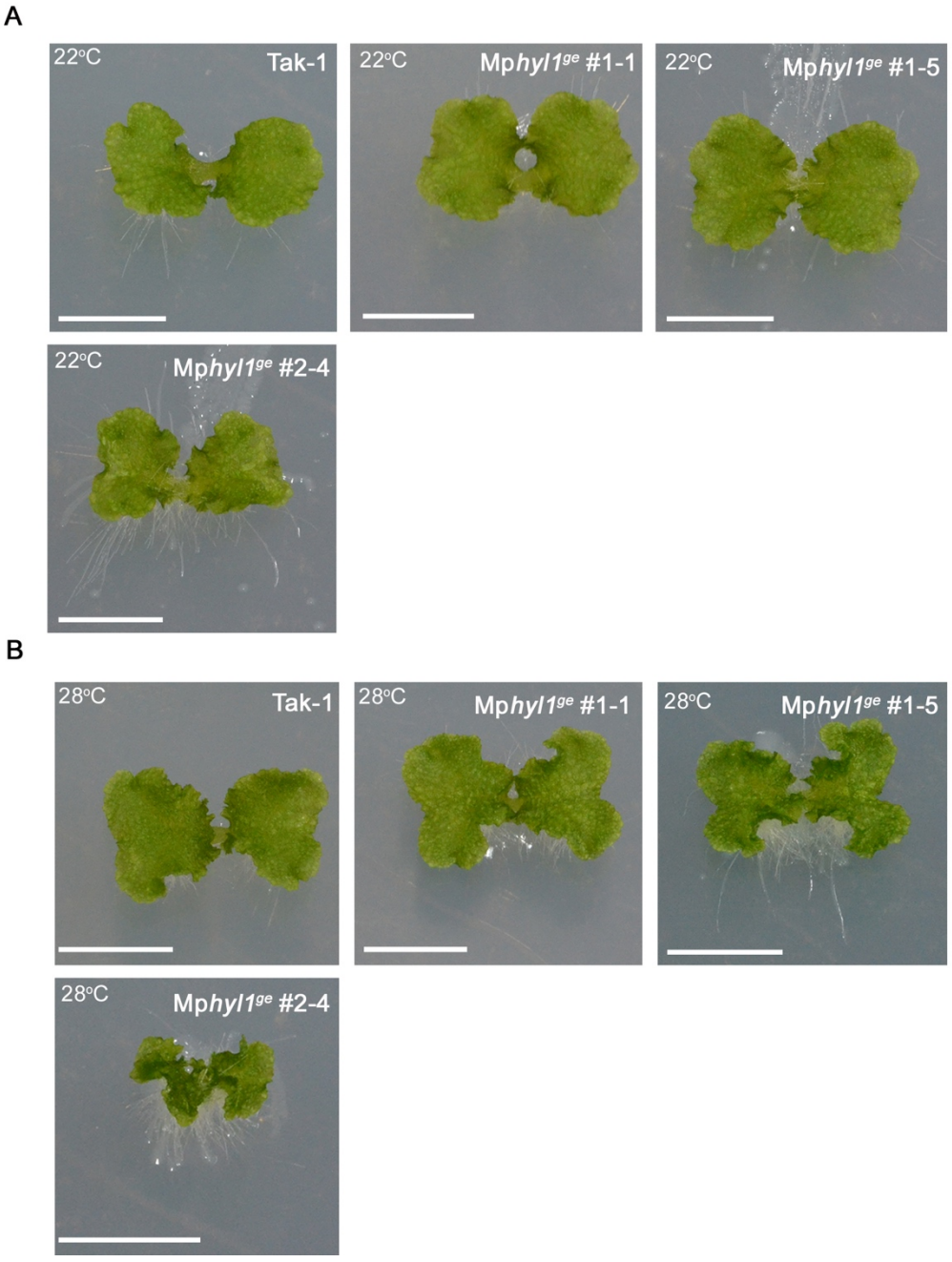

Figure 4. Temperature dependence phenotypic observation of Mp*hyl1*^{ge} plant under **A.** 22°C, 16h light 8h darkness, and **B.** 28°C, 16h light 8h darkness. Bars: 0.5 cm

doi:10.6342/NTU202303945

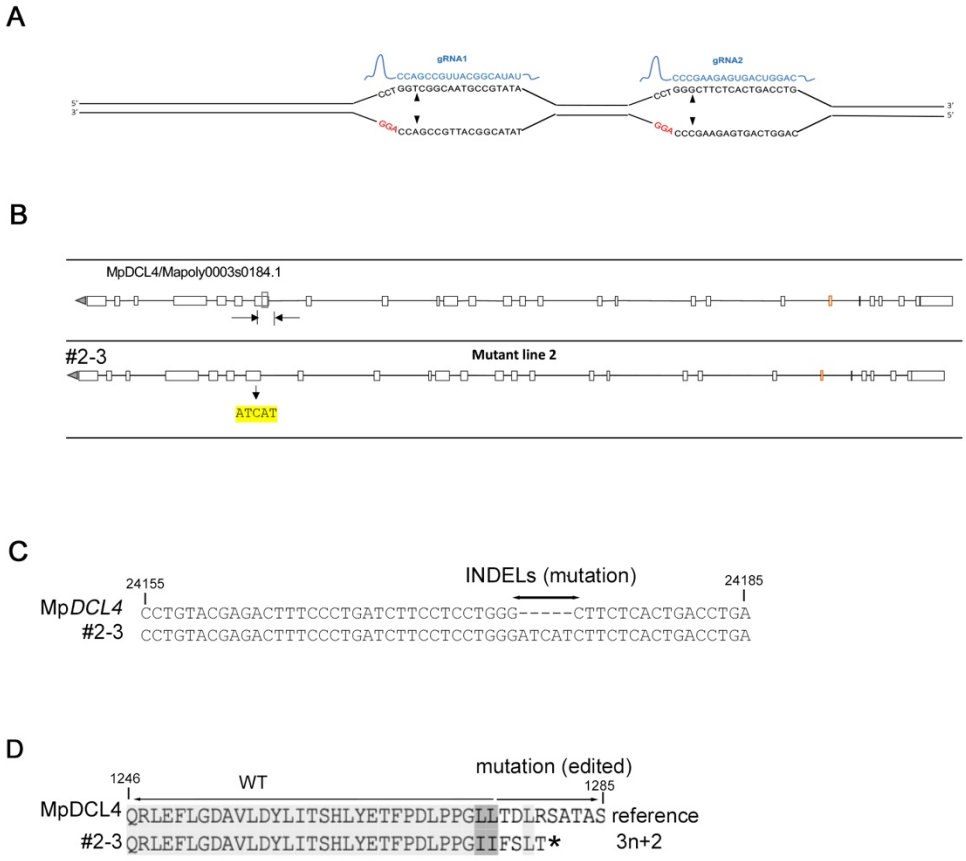

Figure 5. CRISPR-Cas9-mediated mutation on Mp*DCL4*. A. Two gRNAs were designed for Mp*DCL4* gene editing. Red letters show the Protospacer adjacent motif (PAM) sequence. **B.** Genomic structure of Mp*dcl4*^{ge} mutant lines, with CRISPR-Cas9-introduced INDELs of the line. Two small arrows beside the small box represent forward and reverse primers, whereas the small box represents the gRNA targeted line. Highlighted letters represent insertion, and crossed letters represent deletion. The alignment of the **C.** nucleotide. and **D.** amino acid with their references on gRNA2. Wild type (WT) and mutated site were differentiated by arrows. Box indicates the gRNA editing site. 3n + 2 reading frames represent the frameshift.

doi:10.6342/NTU202303945

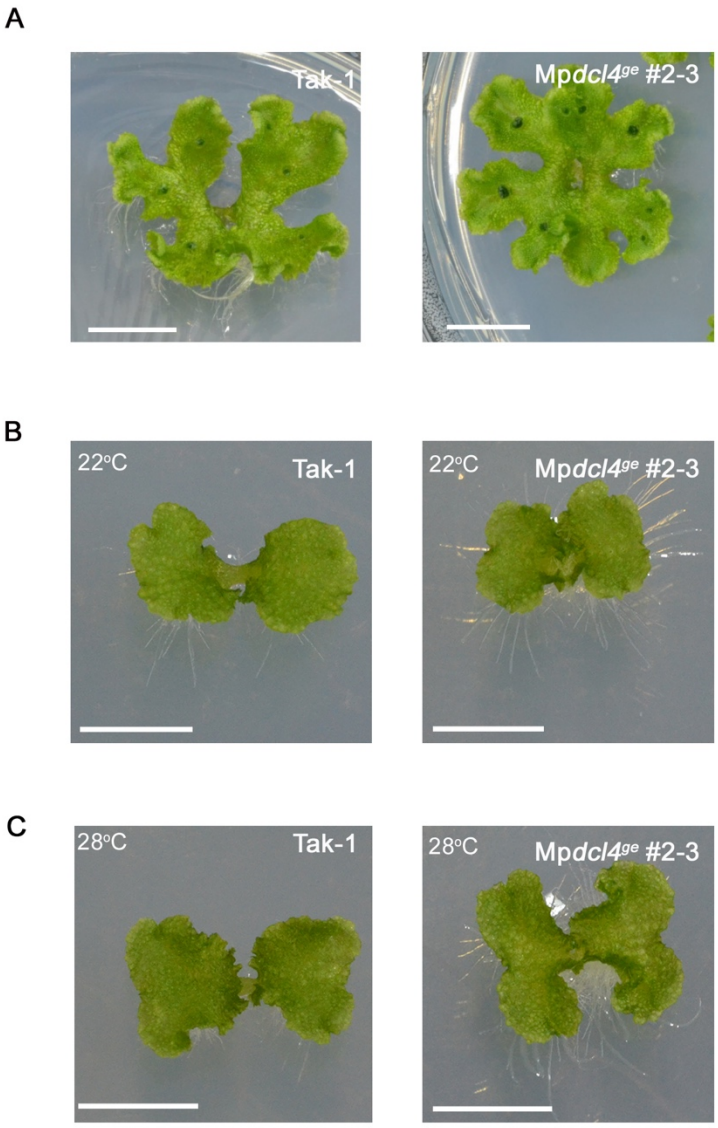

Figure 6. Phenotypic observation of Mp*dcl4*^{ge} mutants under A. normal growth condition**, B.** 22°C, 16h light, 8h darkness, and **C.** 28°C, 16h light, 8h darkness**.** Wild type control: Tak-1. Bars: 0.5 cm

doi:10.6342/NTU202303945

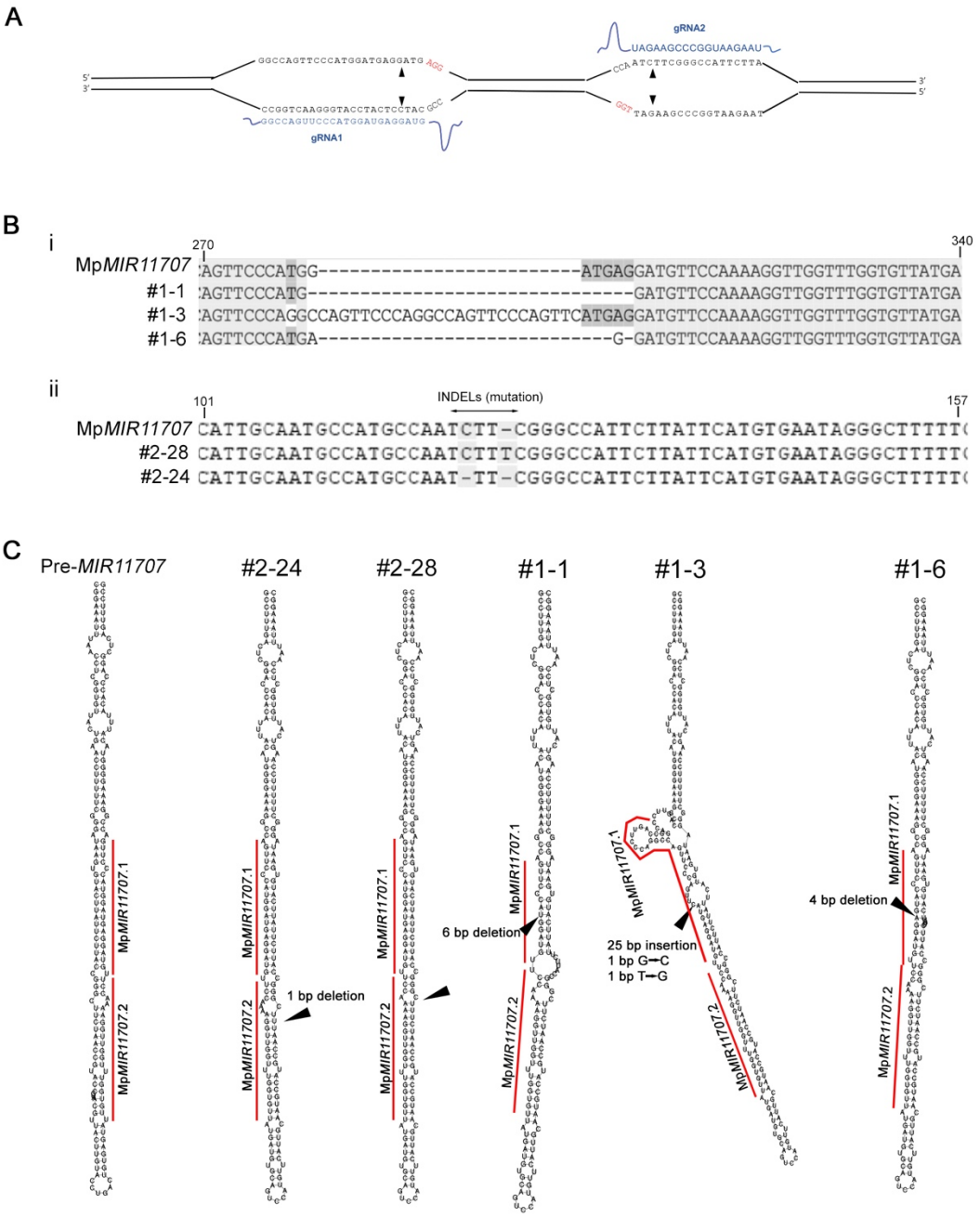

Figure 7. CRISPR-Cas9-mediated mutation on Mp*MIR11707*. A. Two gRNAs were designed for Mp*MIR11707* gene editing. Red letters represent the Protospacer adjacent motif (PAM) sequence. **B.** (i, ii)The alignment of the nucleotide with their references on gRNA1 and gRNA2 respectively. **C.** Predicted precursor of each mutant. Red line indicate position of *MIR11707*.1 and *MIR11707.2*.

doi:10.6342/NTU202303945

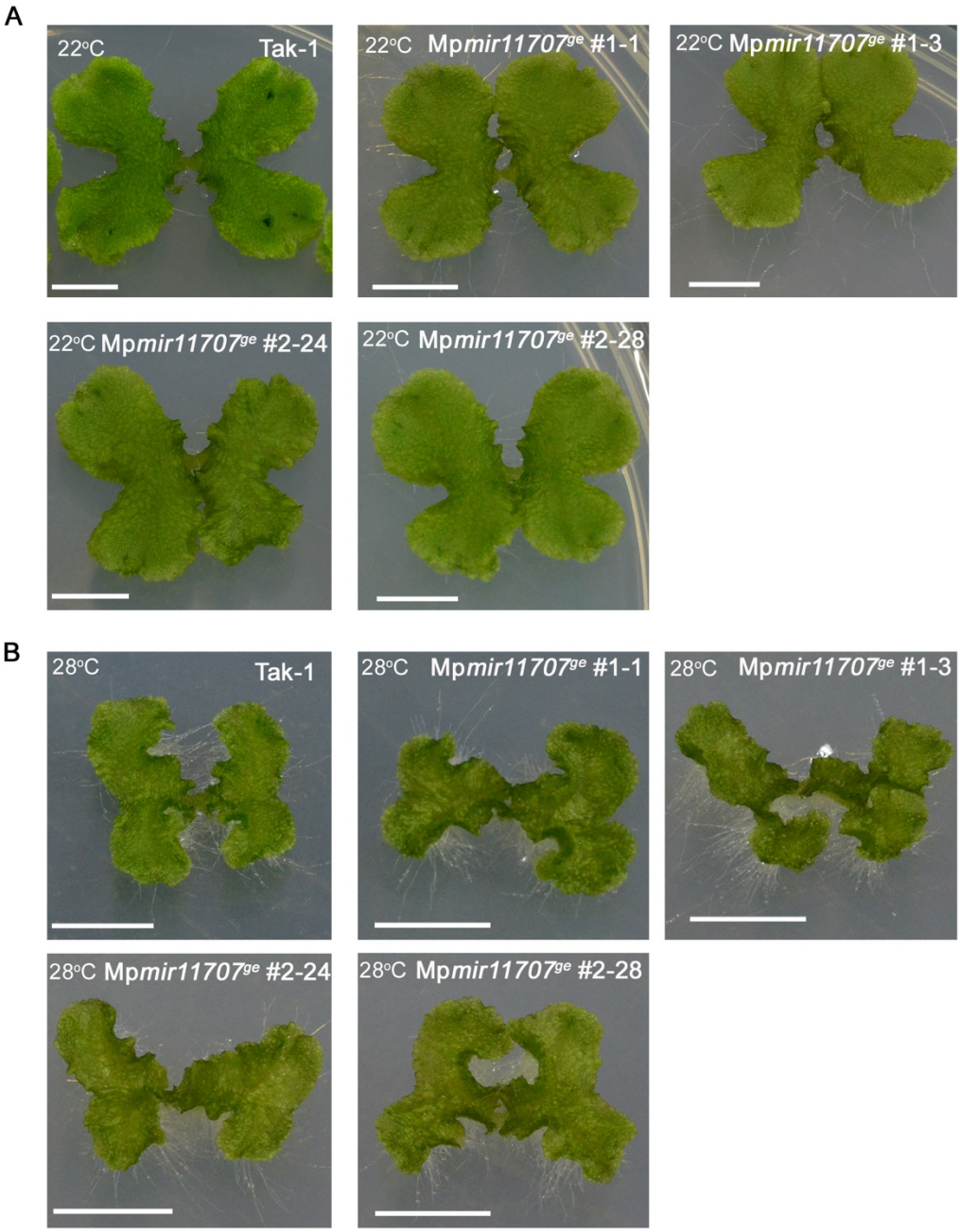

Figure 8. Phenotypic study on Mp*mir11707*^{ge} mutant under **A.** 22°C, 16h light 8h darkness, and **B.** 28°C , 16h light 8h darkness. Bar: 0.5 cm.

doi:10.6342/NTU202303945

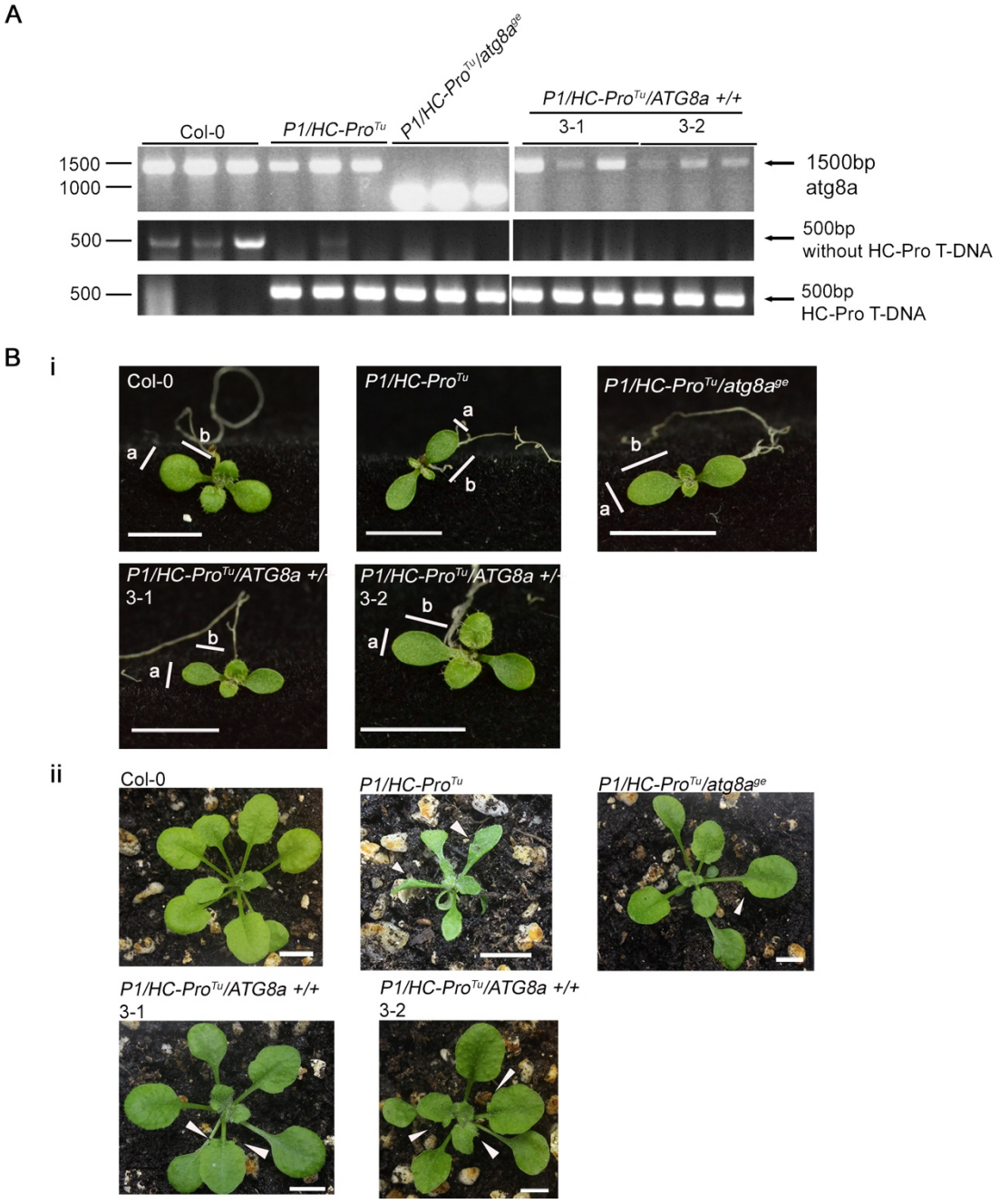

Figure 9. Morphological study of *P1/HC-Pro^{Tu}/atg8a* +/+ transgenic lines taking wild type Col-0, *P1/HC-Pro^{Tu}*, and *P1/HC-Pro^{Tu}/atg8a^{ge}* line as control. A. Genotyping of each transgenic lines with three primers, which targeting atg8a (upper panel) and HC-Pro insertion site (middle and lower panel). Bars: 0.5 cm **B.** Phenotype of transgenic line at (i) 10-day old, and (ii) 21-day old. Bars: 1 cm.

doi:10.6342/NTU202303945

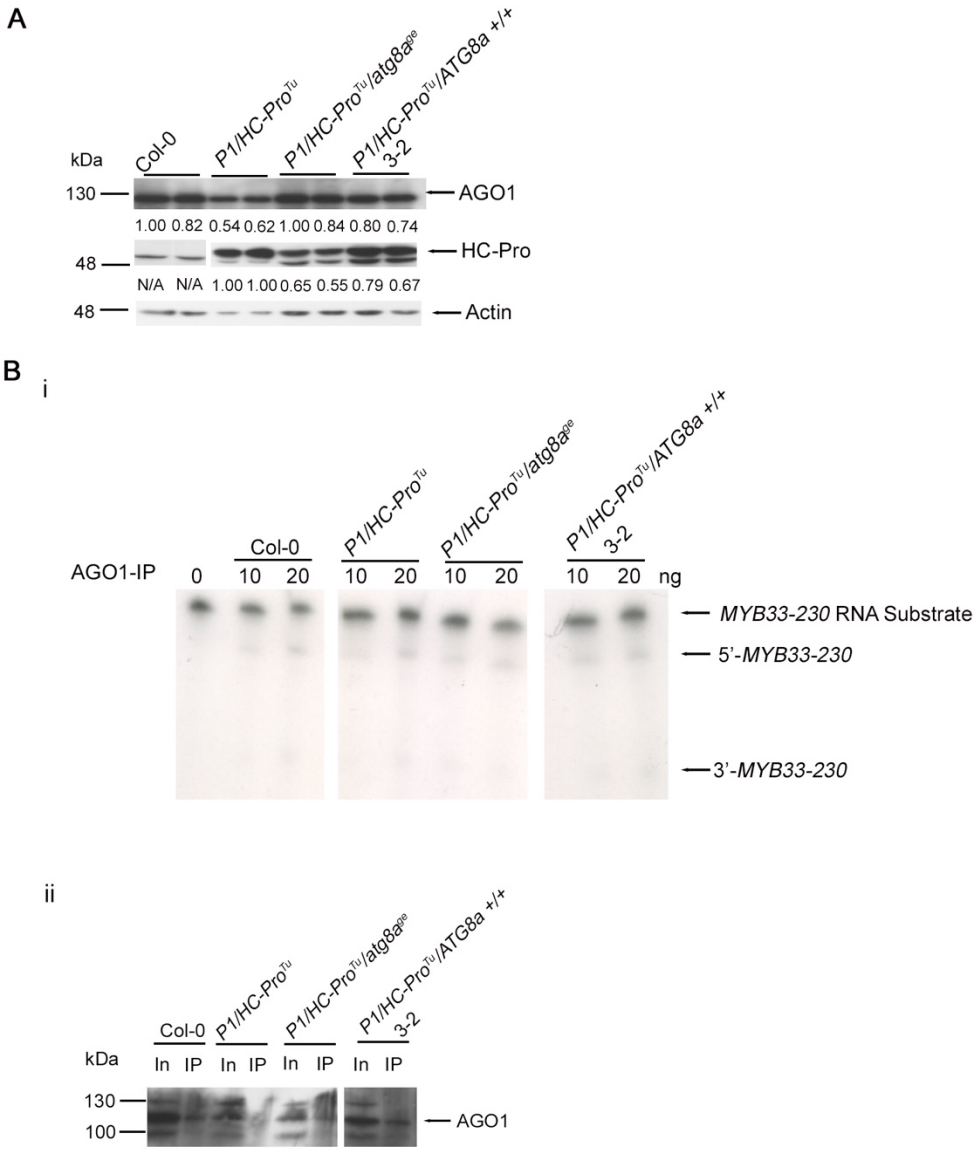

Figure 10. AGO1 studies on *Arabidopsis thaliana P1/HC-Pro^{Tu}/atg8*a +/+ transgenic plant. A. Western blot analysis on HC-Pro and AGO1 in homozygous line. Actin as internal control. **B. (i)** RISC activity assay on *P1/HC-Pro^{Tu}/atg8a*+/+ line. 5' and 3' cleavage is shown as arrow. **(ii)**Western blot analysis showed the existence of AGO1 in all samples. **(iii)** Cleavage efficiency of AGO1 in all samples.

doi:10.6342/NTU202303945

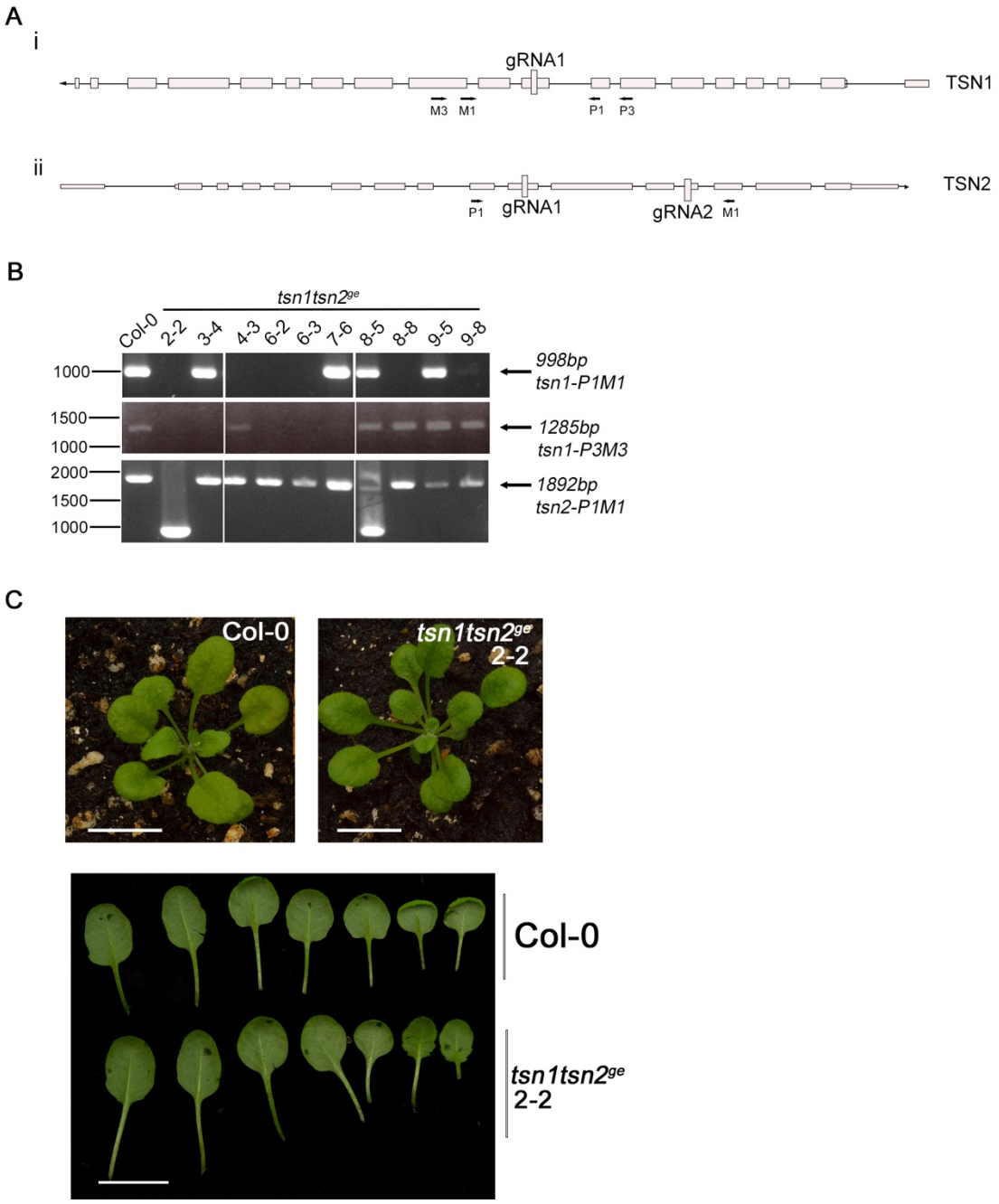

Figure 11. Morphological studies on Arabidopsis thaliana *tsn1tsn2*^{ge} transgenic plant.

A. Schematic diagram indicating position of each primers and gRNAs. **B.** Genotype result on *tsn1tsn2*^{ge} transgenic plant. Succeed transgenic line was expected to be both *TSN1 and TSN2* mutated compared with wild type Col-0. **C.** Phenotype of Col-0 and *tsn1tsn2*^{ge} at 22-day old. Bars: 1 cm.

doi:10.6342/NTU202303945

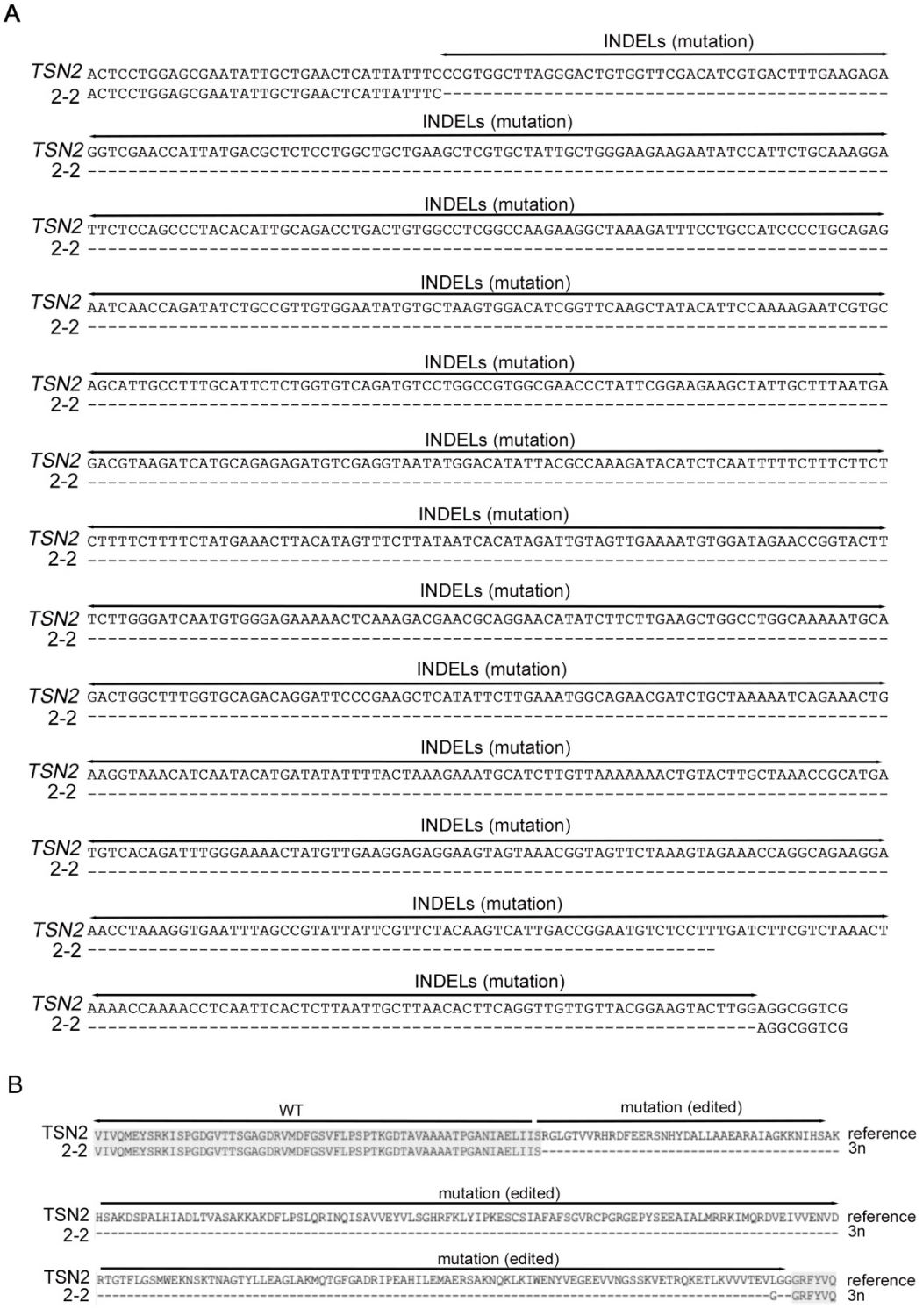

Figure 12. Sequencing result on *tsn1tsn2*^{ge} plant. The alignment of the **A.** nucleotide and **B.** amino acid with their references on TSN2. Wild type (WT) and mutated site were differentiated by arrows. 3n indicates symmetric or in-frame mutation.

doi:10.6342/NTU202303945

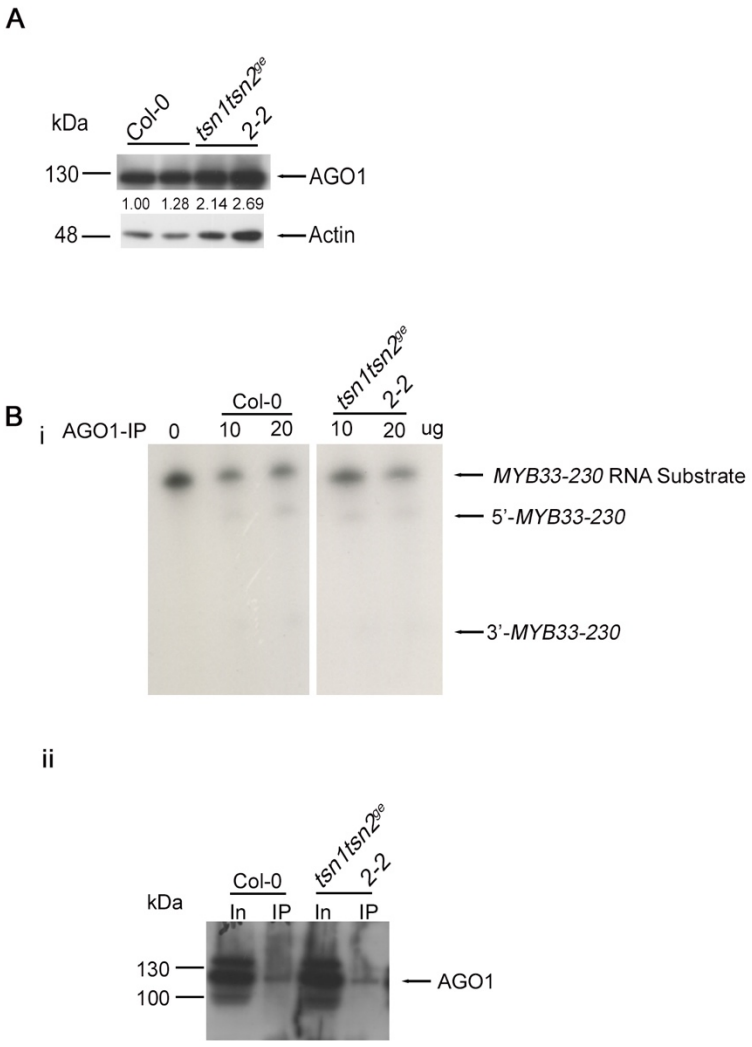

Figure 13. AGO1 studies on *tsn1tsn2*^{ge} mutant line. A. Western blot analysis on AGO1 in homozygous line. Actin as loading control. **B. (i)**RISC activity assay on *tsn1tsn2*^{ge} transgenic plant. 5' and 3' cleavage is shown as arrow. **(ii)**Western blot analysis showed the existence of AGO1 in all samples. **(iii)** Cleavage efficiency of AGO1 in all samples.

doi:10.6342/NTU202303945

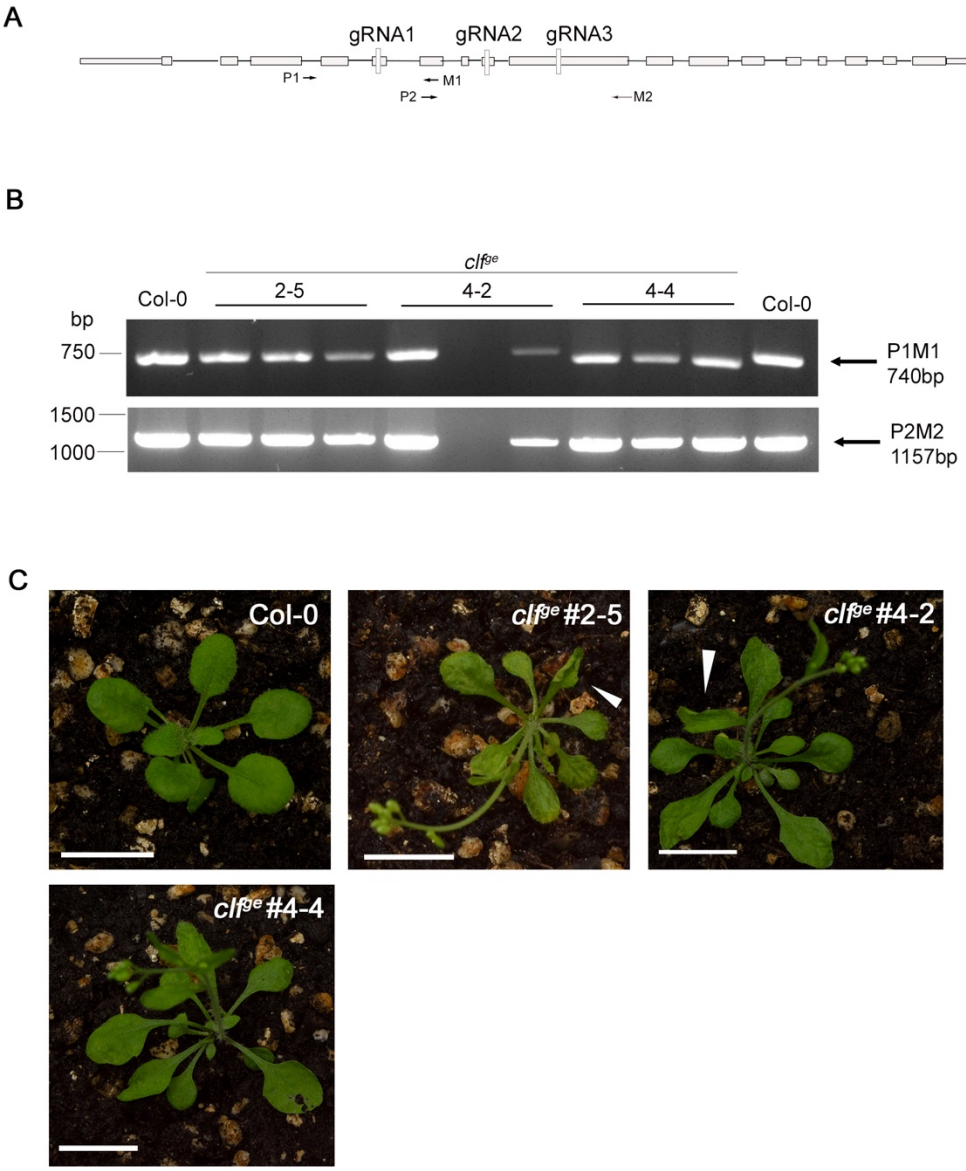

Figure 14. Morphological studies on *Arabidopsis thaliana clf*^{ge} transgenic plant. A. Schematic diagram indicating position of each primers and gRNAs. **B.** Genotype result on *clf*^{ge} transgenic plant. Succeed transgenic line was expected to be *CLF* mutated compared with wild type Col-0. **C.** Phenotype of Col-0 and *clf*^{ge} at 22-day old. Bars: 1 cm.

doi:10.6342/NTU202303945

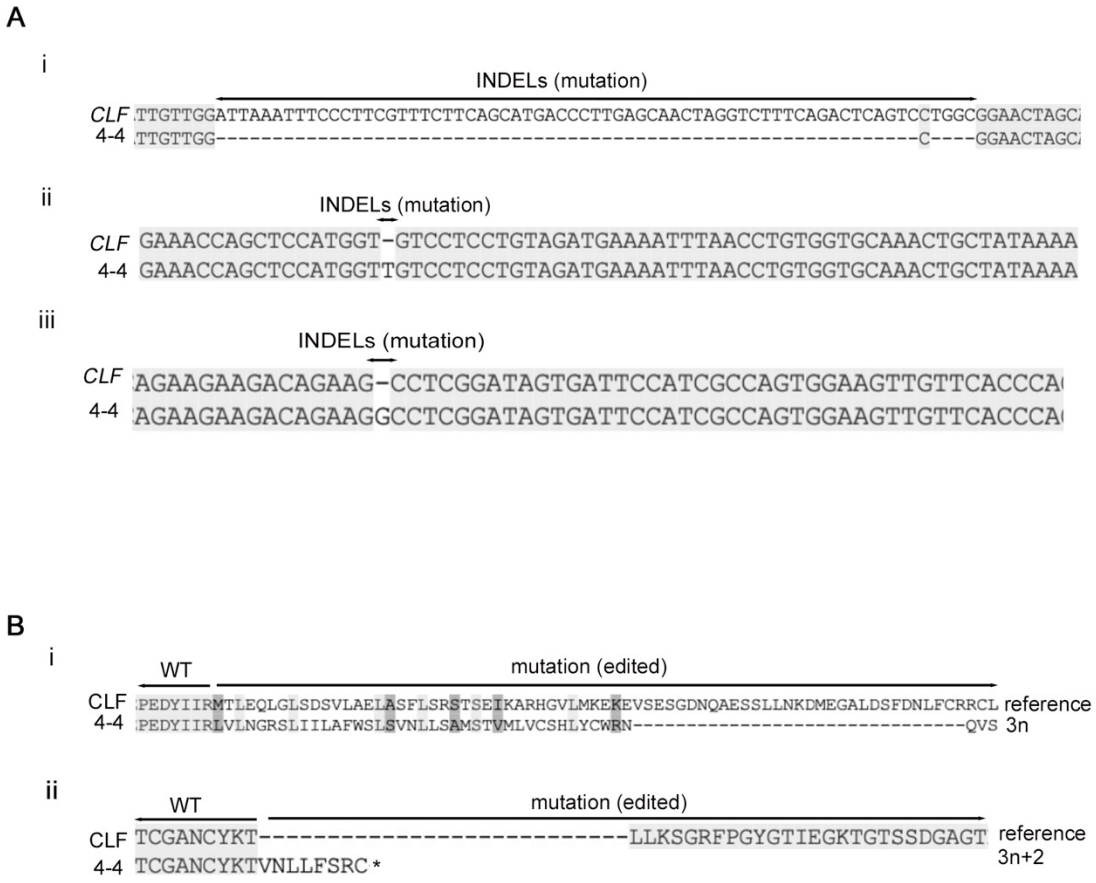

Figure 15. Sequencing result on *clf*^{ge} mutant. The alignment of the **A.** nucleotide. and **B.** amino acid with their references on CLF. Wild type (WT) and mutated site were differentiated by arrows. 3n + 2 reading frames represent the frameshift or asymmetric mutation.

doi:10.6342/NTU202303945

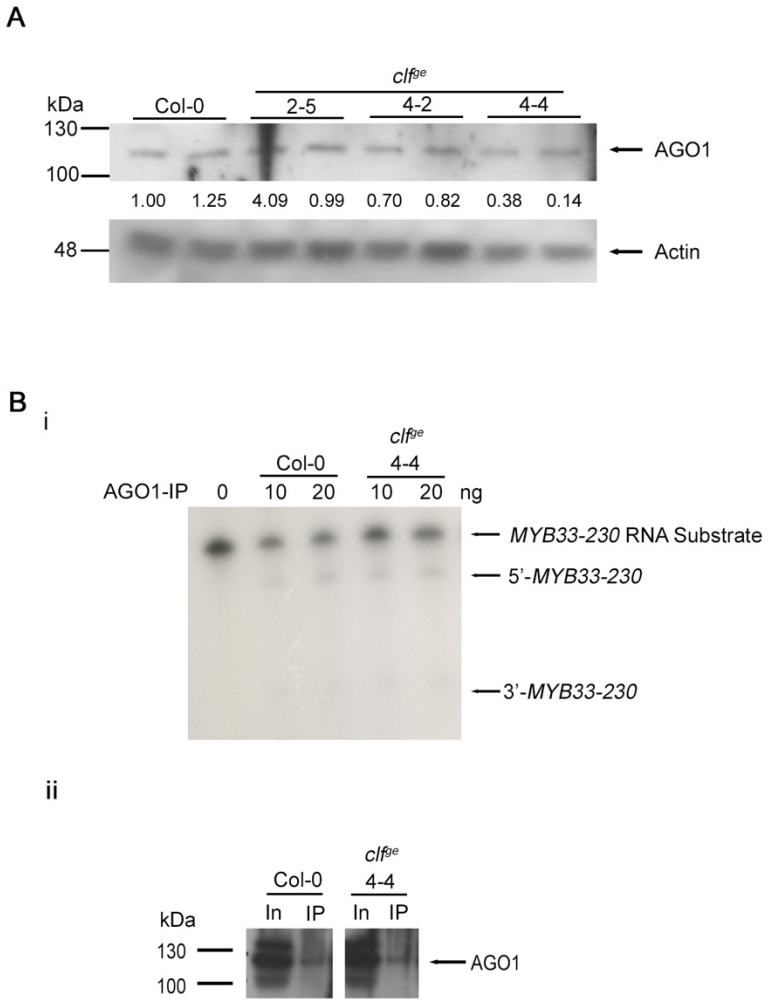

Figure 16. AGO1 activity studies on *clf*^{ge} mutant line. A. Western blot analysis on AGO1 in homozygous line. Actin as internal control. **B.** (i)RISC activity assay on *clf*^{ge} transgenic plant. 5' and 3' cleavage is shown as arrow. (ii)Western blot analysis showed the existence of AGO1 in all samples.

doi:10.6342/NTU202303945

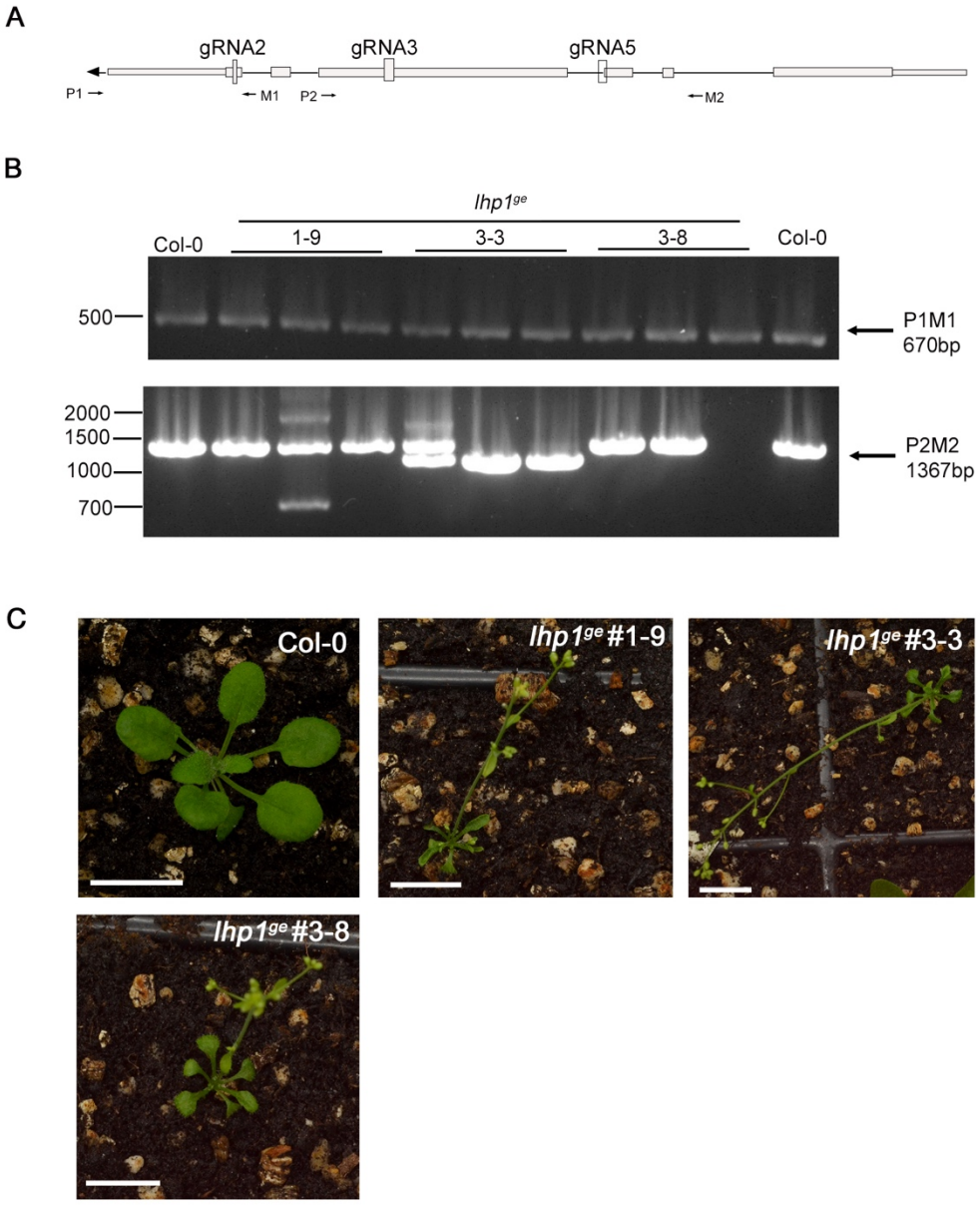

Figure 17. Morphological studies on Arabidopsis thaliana *lhp1*^{ge} transgenic plant. A. Schematic diagram indicating position of each primers and gRNAs. **B.** Genotype result on *lhp1*^{ge} transgenic plant. Succeed transgenic line was expected to be *LHP1* mutated compared with wild type Col-0. **C.** Phenotype of Col-0 and *lhp1*^{ge} at 22-day old. Bars: 1 cm.

doi:10.6342/NTU202303945

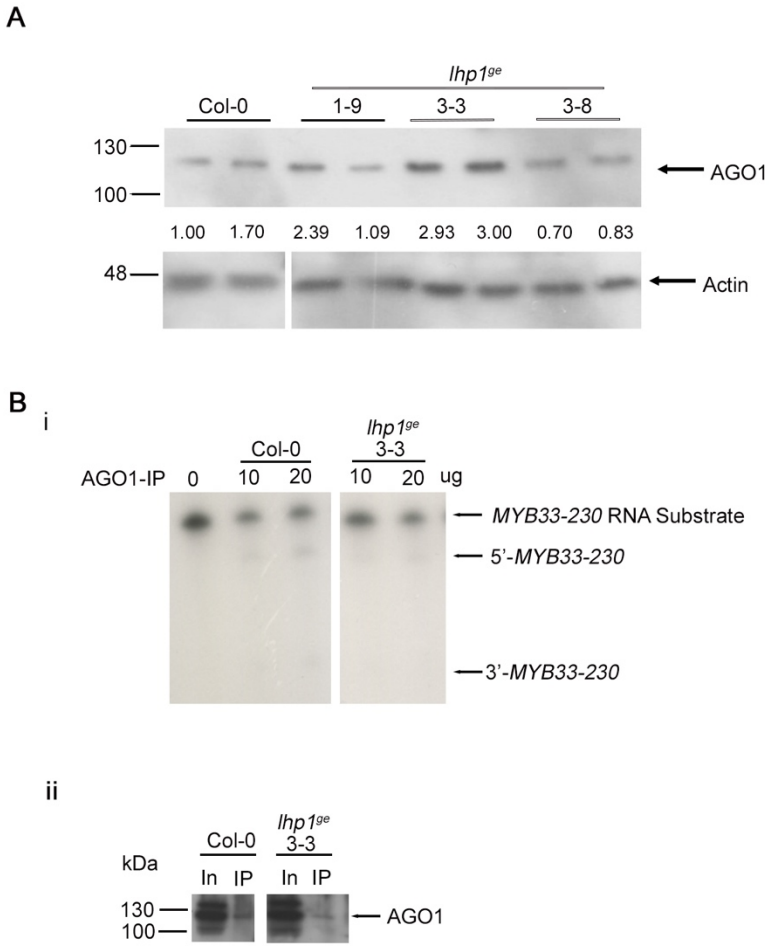

Figure 18. AGO1 activity studies on *lhp1*^{ge} mutant line. A. Western blot analysis on AGO1 in homozygous line. Actin as internal control. **B.** (i)RISC activity assay on *lhp1*^{ge} transgenic plant. 5' and 3' cleavage is shown as arrow. (ii)Western blot analysis showed the existence of AGO1 in all samples. (iii) Cleavage efficiency of AGO1 in all samples.

doi:10.6342/NTU202303945